

THE VALIDITY OF THE NORDHEIM-GORTER
RULE WHEN MAGNETIC SCATTERING IS PRESENT

by

DAVID RALPH KARECKI

B.Sc., Michigan State University, 1968

A THESIS SUBMITTED IN PARTIAL FULFILLMENT OF
THE REQUIREMENTS FOR THE DEGREE OF
MASTER OF SCIENCE

in the Department

of

Physics

© DAVID RALPH KARECKI 1972
SIMON FRASER UNIVERSITY
September 1972

APPROVAL

Name: David Ralph Karczcki
Degree: Master of Science
Title of Thesis: The Validity of the Nordheim-Gorter Rule
When Magnetic Scattering is Present

Examining Committee:

Chairman: K.E. Rieckhoff

D.J. Huntley
Senior Supervisor

S. Gyax

D. Dunn

F.J. Blatt

Date Approved: September 6, 1972

ABSTRACT

Small amounts of Sn, 200 to 5000 ppm, were added to Au+.03 at .% Fe thermocouple wire. The thermopower of these alloys was measured from helium to room temperatures. Below 100K, the Nordheim-Gorter rule fits the data well even though the conditions for its validity are not strictly obeyed. This justifies use of the Nordheim-Gorter rule when inelastic spin-flip scattering contributes to the thermopower.

An appendix describes the search for superconducting behavior of Pb impurities in Au-Fe and pure Au wires through magnetoresistance and magnetothermopower measurements. None was found. This disagrees with some results of Walker (1971).

TABLE OF CONTENTS

LIST OF FIGURES	v
LIST OF TABLES	vi
ACKNOWLEDGMENTS	vii
I. INTRODUCTION	1
I-1 Standard Transport Theory	3
I-2 The Connection Between Thermal Resistivity and Thermopower	15
I-3 Kondo's Expression for the Thermopower of Dilute Magnetic Alloys	19
I-4 Application of the Nordheim-Gorter Rule to Experiment	22
I-5 The Effect of Phonon Drag	24
I-6 The Effect of Anisotropy on the Validity of the Nordheim-Gorter Rule	26
II. EXPERIMENTAL	38
II-1 Sample Preparation	38
II-2 Thermopower Measurement	41
III. EXPERIMENTAL RESULTS	47
III-1 The Thermopower of <u>Au</u> -Fe-Sn Alloys	47
III-2 The Resistivity of <u>Au</u> -Fe-Sn Alloys	48
III-3 The Nordheim-Gorter Plots	49
IV. DISCUSSION AND CONCLUSIONS	55
APPENDIX I: The Diffusion of Sn in Solid Au ...	59
APPENDIX II: The Validity of Matthiessen's Rule in Ternary Alloys	62
APPENDIX III: The Effect of Superconducting Pb Impurities on the Magnetothermo- power and Magnetoresistance of Pure Au and <u>Au</u> -Fe Alloys	69
LIST OF REFERENCES	84

LIST OF FIGURES

<u>Figure</u>	<u>Page</u>
1.1 Absolute thermopower of several dilute gold-iron alloys	30
1.2 The thermoelectric power of Au-Fe alloys for various Fe concentrations	31
1.3 Lorentz ratio plotted against temperature	32
1.4 Nordheim-Gorter plot of various dilute alloys of copper	33
1.5 Absolute thermoelectric power of dilute Au-Sn alloy at 1K as function of inverse residual resistance ratio	34
1.6 Modified Nordheim-Gorter plots at 290K for solid solutions of gallium, Germanium, and arsenic in copper	35
1.7 Percent deviation from Matthiessen's rule at 290K as a function of residual resistivity for Ca-Ga, Cu-Ge, and Cu-As alloys	35
1.8 Absolute thermopower of some pure noble metals ...	36
1.9 Nordheim-Gorter plots for dilute Ag alloys at 300K	37
2.1 Lower portion of apparatus	42
3.1a Absolute thermopower of <u>Au-Fe-Sn</u> alloys versus temperature	50
3.1b Absolute thermopower of <u>Au-Fe-Sn</u> alloys versus temperature	51
3.2 Low temperature Nordheim-Gorter plots for <u>Au-Fe-Sn</u> alloys	52
3.3 Nordheim-Gorter plot of <u>Au-Fe-Sn</u> alloys at 25K ...	53
3.4 Nordheim-Gorter plots of <u>Au-Fe-Sn</u> alloys at intermediate temperatures	54
I.1 Concentration vs. radial position for various times for diffusion into cylinder from the surface	61
II.1 $\Delta(T)/\rho_j(0)$ versus temperature for various gold alloys	66
II.2 Same as II.1	66

<u>Figure</u>	<u>Page</u>
II.3 Temperature dependence of the solute contribution Fe to the resistivity of gold-iron alloys in the range 4 to 1000K	67
II.4 Deviations from Matthiessen's rule versus temperature for various alloys	68
III.1 Percentage change in thermopower versus magnetic field in <u>Au+0.03</u> at .% Fe at low fields	70
III.2 Magnetic field H_c at middle of step anomaly vs. temperature T in <u>C</u> Au-Fe alloy	71
III.3 Magnetoresistance of Walker's <u>Au+0.03</u> at .% Fe alloy at T = 4.2K	74
III.4 Magnetoresistance of April 1971 <u>Au+0.03</u> at .% Fe alloy at T = 4.2K	75
III.5 Reduced Kohler plot of Au and Au-Pb alloys	76
III.6 Magnetothermopower of Walker's <u>Au+0.03</u> at .% Fe alloy of T = 4.2K versus Ag normal	78
III.7 Magnetothermopower of <u>Au+0.03</u> at .% Fe + ~ 1100 ppm Pb at T = 4.2K versus Ag normal	79

LIST OF TABLES

<u>Table</u>	<u>Page</u>
I Residual Resistance and Approximate Sn Concentrations of the Au-Fe-Sn Specimens	40

ACKNOWLEDGMENTS

I would like to thank my examining committee, especially Dr. D.J. Huntley, both for assistance in performing the experiment and in writing this thesis. Thanks also are in order for Mrs. Barbara McKellar who typed the manuscript. The financial support of the National Research Council and the Simon Fraser University Department of Physics is gratefully acknowledged.

CHAPTER I

INTRODUCTION

The thermopower of Au-Fe alloys has been extensively covered in the literature. One particular aspect, however, has not received much attention. Referring to Figure 1.1 (Berman et al. 1964) and Figure 2 (Berman and Kopp 1971) one sees the characteristic Kondo peak and also that the temperature of this peak is not particularly concentration dependent. However, the magnitude of this peak is different for alloys of similar concentration, especially Au+~.03 at .% Fe.

The usual explanation of this feature is to invoke the Nordheim-Gorter rule. Nordheim and Gorter (1935) proposed the following rule for the observed thermopower, S , in metals where different electron scattering mechanisms are present:

$$S = \frac{\sum_i \rho_i S_i}{\sum_i \rho_i} \quad (1.1)$$

S_i and ρ_i are the characteristic thermopower and electrical resistivity respectively due to the i -th scattering mechanism. In Au-Fe there are three scattering mechanisms: non-Fe impurities and imperfections, phonons, and Fe. Since the thermopower of pure Au (Figure 1.8) is small at low temperatures, and the lattice resistivity is also small, equation (1.1) reduces to

$$S = \frac{\rho_{Fe} S_{Fe}}{\rho_{Fe} + \rho_{imp}}$$

assuming $\frac{\rho_{imp} S_{imp}}{\rho_{Fe} + \rho_{imp}}$ is small.

Thus if some of the iron present is oxidized the observed thermopower will be reduced in magnitude, assuming that the rule is indeed valid. Since the rule has not been experimentally verified for alloys of this type, we did the following experiment.

This thesis deals with the validity of the Nordheim-Gorter rule for Au+0.03 at .% Fe with added Sn impurities. The Au-Fe is commercially available in wire form as a thermocouple element, and Sn is readily introduced into the wire. The thermopowers of such alloys were measured from He to room temperatures for Sn concentrations of about 200 ppm to 5000 ppm. Before describing the experiment, however, it is worthwhile to go through the derivation of the Nordheim-Gorter rule keeping track of the assumptions made.

I-1 Standard Transport Theory

Let $f(\underline{k}, \underline{r}, t)$ be the probability of finding an electron in a state with wavevector \underline{k} at position \underline{r} at time t , the distribution function. \underline{k} is the electron wavevector and \underline{r} is the position. In the absence of collisions, the equation of continuity for f may be written

$$\begin{aligned} \frac{\partial f}{\partial t} &= - \frac{\partial}{\partial \underline{r}} \cdot \left(f \frac{\partial \underline{r}}{\partial t} \right) - \frac{\partial}{\partial \underline{k}} \cdot \left(f \frac{d\underline{k}}{dt} \right) \\ &= - \underline{v} \cdot \frac{\partial f}{\partial \underline{r}} - \frac{d\underline{k}}{dt} \cdot \frac{\partial f}{\partial \underline{k}} - f \left[\frac{\partial}{\partial \underline{r}} \cdot \underline{v} + \frac{\partial}{\partial \underline{k}} \cdot \frac{d\underline{k}}{dt} \right] \end{aligned}$$

For Bloch electrons $\hbar v = \text{grad}_{\underline{k}} E$ is independent of position, and $d\underline{k}/dt = (e/\hbar) (\underline{E} + (1/c)\underline{v} \times \underline{H})$ involves \underline{k} only through a gradient, leaving

$$\frac{\partial f}{\partial t} = - \underline{v} \cdot \frac{\partial f}{\partial \underline{r}} - \frac{d\underline{k}}{dt} \cdot \frac{\partial f}{\partial \underline{k}}$$

To this is added a collision term. In the steady state $\frac{\partial f}{\partial t} = 0$, and what remains is the Boltzmann equation,

$$\left. \frac{\partial f}{\partial t} \right)_{\text{scatt.}} = \underline{v} \cdot \frac{\partial f}{\partial \underline{r}} + \frac{d\underline{k}}{dt} \cdot \frac{\partial f}{\partial \underline{k}} \quad (1.2)$$

To simplify solving this equation, it is common to linearize it, taking only the first non-vanishing terms assuming the departure from equilibrium is small. f is assumed to vary with position only through temperature gradients.

$$\underline{v} \cdot \frac{\partial f}{\partial \underline{r}} = \underline{v} \cdot \frac{\partial f}{\partial T} \frac{\partial T}{\partial \underline{r}} \cong \underline{v} \cdot \frac{\partial f^{\circ}}{\partial T} \frac{\partial T}{\partial \underline{r}}$$

f° is the equilibrium distribution function for Fermi-Dirac statistics. The term due to external fields can also be

simplified to first order

$$\frac{\partial f}{\partial \underline{k}} \cong \frac{\partial f^0}{\partial \underline{k}} = \frac{\partial f^0}{\partial E} \cdot \frac{\partial E}{\partial \underline{k}} = \hbar \underline{v} \frac{\partial f^0}{\partial E}$$

since f^0 is a function of energy and temperature only. If a magnetic field were present this approximation would vanish ($\underline{v} \cdot (\underline{v} \times \underline{H}) = 0$), but only the case of no magnetic field will be considered here. With these approximations, one has the linearized Boltzmann equation,

$$\left(\frac{\partial f}{\partial t} \right)_{\text{scatt.}} = \underline{v} \cdot \left(\frac{\partial f^0}{\partial T} \frac{\partial T}{\partial \underline{r}} + e \underline{E} \frac{\partial f^0}{\partial E} \right) \quad (1.3).$$

where it is implicit that only the first order terms in deviation from equilibrium will be considered in the collision term, the higher order terms on the right having already been neglected.

Three types of scattering processes will be considered here: normal impurity scattering (elastic), the electron-phonon interaction, and magnetic spin-flip scattering. All these play a role in the Au-Fe-Sn system studied.

(a) Elastic Scattering

Here the probability of an electron being scattered from state \underline{k} to \underline{k}' in the range $d\underline{k}'$ is given by

$$p(\underline{k}, \underline{k}') d\underline{k}' = f(1-f') Q(\underline{k}, \underline{k}') d\underline{k}'$$

where $Q(\underline{k}, \underline{k}')$ is the intrinsic scattering probability neglecting Fermi statistics. The inverse process is

$$p(\underline{k}', \underline{k}) d\underline{k}' = f'(1-f) Q(\underline{k}', \underline{k}) d\underline{k}'$$

f and f' are the distribution functions for the regions of \underline{k} space being considered in the collision. By the principle of microscopic reversibility, $Q(\underline{k}, \underline{k}') = Q(\underline{k}', \underline{k})$ so that the total transition rate is given by

$$\begin{aligned} \left. \frac{\partial f}{\partial t} \right)_{\text{scatt.}} &= \int [f(1-f') - f'(1-f)] Q(\underline{k}, \underline{k}') d\underline{k}' = \\ &= \int [(f-f^{\circ}) - (f'-f^{\circ}')] Q(\underline{k}, \underline{k}') d\underline{k}' \quad (1.4) \end{aligned}$$

since $f^{\circ} = f^{\circ}'$ when scattering is elastic. f° and f°' are the distribution functions at equilibrium in the absence of external gradients. Note that this equation contains only first order deviations from equilibrium. It is sometimes convenient to make a formal transformation of equation (1.4) by defining a function ϕ such that $f-f^{\circ} = \phi \partial f^{\circ} / \partial E$. Then the scattering term is in the so-called canonical form,

$$\left. \frac{\partial f}{\partial t} \right)_{\text{scatt.}} = \frac{1}{kT} \int (\phi - \phi') P(\underline{k}, \underline{k}') d\underline{k}' \quad (1.5)$$

where $P(\underline{k}, \underline{k}')$ is the equilibrium transition rate,

$$Q(\underline{k}, \underline{k}') f^{\circ} (1-f^{\circ}).$$

(b) The Electron-phonon Collision Term

Here the scattering term depends on the phonon distribution function, $N_{\underline{q}}$. In the scattering process a phonon is either created or destroyed. The number of electrons scattered out of \underline{k} per unit time is

$$\begin{aligned} \iint [f(1-f') (N_{\underline{q}} + 1) Q_{\underline{k}}^{\underline{q}k'} + f(1-f') N_{\underline{q}} Q_{\underline{k}q}^{\underline{k}'}] d\underline{k}' d\underline{q} = \\ \iint f(1-f') [(n_{\underline{q}} + 1) Q_{\underline{k}}^{\underline{q}k'} + N_{\underline{q}} Q_{\underline{k}q}^{\underline{k}'}] d\underline{k}' d\underline{q} \end{aligned}$$

Similarly for inverse processes,

$$\iint f'(1-f) \left[(N_{\underline{q}}+1) Q_{\underline{k}}^{\underline{qk}'} + N_{\underline{q}} Q_{\underline{k}',\underline{q}}^{\underline{k}} \right] dk' d\underline{q}$$

In the absence of external fields all these processes should yield no net gain or loss of electrons in any volume element of phase space. Applying the principle of detailed balance one obtains

$$f^0(1-f^{0'}) \left[N_{\underline{q}}^0 + 1 \right] Q_{\underline{k}}^{\underline{qk}'} - f^{0'}(1-f^0) N_{\underline{q}}^0 Q_{\underline{k}',\underline{q}}^{\underline{k}} = 0$$

These two equations can be combined in a manner analogous to the following section to give

$$\left(\frac{\partial f}{\partial t} \right)_{\text{scatt.}} = \frac{1}{kT} \left\{ \iint \left[(\phi_{\underline{k}} + \phi_{\underline{q}} - \phi_{\underline{k}'}) P_{\underline{kq}}^{\underline{k}'} + (\phi_{\underline{k}} - \phi_{\underline{q}} - \phi_{\underline{k}'}) P_{\underline{k}}^{\underline{qk}'} \right] dk' d\underline{q} \right\}$$

to first order in deviations from equilibrium where $P_{\underline{k},\underline{q}}^{\underline{k}'}$ is the total transition probability when a phonon is destroyed.

The presence of the phonon distribution function in this formula represents the coupling of the two Boltzmann equations for electrons and phonons. This obviously intractable situation is remedied by making the Bloch assumption: In metals, the phonons are in thermal equilibrium. That is, $\phi_{\underline{q}} = 0$. This means that the phonons carry no heat. This is not the case when phonon drag effects are observed in the thermopower.

(c) Magnetic Spin-flip Scattering

Kondo (1965) provided the first satisfactory explanation

for the anomalously large thermopower of dilute magnetic alloys. He considered all the first order processes that could happen to an electron with spin scattering off a transition metal impurity with spin and a localized magnetic field, H_n . A scattered electron can have its spin flipped or, left alone while the Zeeman energy of the scattering magnetic impurity may be increased, decreased or unchanged.

Symbolically, $\underline{k}\pm \rightarrow \underline{k}'\pm$ and $\underline{k}\pm M_n + 1$, where \pm denotes the spin direction of the carrier electron and M_n denotes the component of the impurity spin in the localized magnetic field.

There are twelve such processes, and assuming that the scattering is isotropic,

$$\begin{aligned} \left. \frac{\partial f}{\partial t} \right)_{\text{scatt.}} = & \sum_{\underline{k}'} \left\{ W(\underline{k}' + \rightarrow \underline{k}\pm) + W(\underline{k}' - \rightarrow \underline{k}\pm) \right\} (f' - f) + \\ & + \sum_{\underline{n}\underline{k}} \left\{ W(\underline{k}' + M_n \rightarrow \underline{k} + M_n + 1) + W(\underline{k}' - M_n \rightarrow \underline{k} + M_n + 1) \right\} f'(1-f) \\ & - \sum_{\underline{n}\underline{k}'} \left\{ W(\underline{k} + M_n \rightarrow \underline{k}' + M_n - 1) + W(\underline{k} + M_n \rightarrow \underline{k}' - M_n - 1) \right\} f(1-f') \\ & + (\text{similar terms}) \end{aligned}$$

The first term describes processes where there is no change in the Zeeman energy. This scattering is elastic and analogous to the expression of part (a). The other term can be simplified.

Consider inverse processes such as

$$\sum_{\underline{n}\underline{k}'} \left\{ W(\underline{k}' - M_n \rightarrow \underline{k} + M_n + 1) f' (1-f) - W(\underline{k} + M_n \rightarrow \underline{k}' - M_n + 1) f (1-f') \right\}$$

At equilibrium detailed balance requires that this term vanish.

$$\sum_n W(\underline{k}' - M_n \rightarrow \underline{k} + M_n + 1) f^{0'} (1-f^0) - W(\underline{k} + M_n \rightarrow \underline{k}' - M_n + 1) f^0 (1-f^{0'}) = 0$$

This eliminates four of the transition probabilities giving an expression like

$$\sum_{\underline{n}\underline{k}'} W(\underline{k}' - M_n \rightarrow \underline{k} + M_n + 1) \left\{ f' (1-f) - \frac{f^{0'} (1-f^0)}{f^0 (1-f^{0'})} f (1-f') \right\} =$$

$$\sum_{\underline{n}\underline{k}'} W(\underline{k}' - M_n \rightarrow \underline{k} + M_n + 1) \left\{ f^{0'} (1-f^0) \left[\frac{f' (1-f)}{f^0 (1-f^0)} - \frac{f (1-f')}{f^0 (1-f^{0'})} \right] \right\}$$

This can be simplified to terms first order in $f-f^0$. (Van Peski-Timbergen 1963).

$$\sum_{\underline{n}\underline{k}'} W(\underline{k}' - M_n \rightarrow \underline{k} + M_n + 1) f^{0'} (1-f^0) \left\{ \frac{f' - f^{0'}}{f^{0'} (1-f^{0'})} - \frac{f - f^0}{f^0 (1-f^0)} \right\} \quad (1.6)$$

For spherical Fermi surfaces where a relaxation time exists, the Boltzmann equation has a solution of the form

$$f = f^0 - k\chi F(E) \frac{\partial f^0}{\partial E} \quad (1.7)$$

with electric fields and temperature gradients in the x - direction. (Wilson 1953, p. 210). This makes $f - f^0$ an odd function of k so that the primed term in equation (1.6) vanishes when summed over \underline{k}' . What is left is just

$$\sum_{\underline{n}\underline{k}'} \frac{f^{0'}}{f^0} (f - f^0) W(\underline{k}' - M_n \rightarrow \underline{k} + M_n + 1)$$

Kondo's final expression then reads

$$\left. \frac{\partial f}{\partial t} \right)_{\text{scatt.}} = -\frac{(f - f^0)}{\tau(E)}$$

$$1/\tau(E) = \sum_{\underline{k}'} [W(\underline{k}' \rightarrow \underline{k} +) + W(\underline{k}' \rightarrow \underline{k} +)]$$

$$\sum_{\underline{n}\underline{k}'} \frac{f^{0'}}{f^0} \left\{ W(\underline{k}' + M_n \rightarrow \underline{k} + M_n + 1) + W(\underline{k}' - M_n \rightarrow \underline{k} + M_n + 1) \right\}$$

$$\sum_{\underline{n}\underline{k}'} \frac{f^{0'}}{f^0} \left\{ W(\underline{k}' + M_n \rightarrow \underline{k} + M_n - 1) + W(\underline{k}' - M_n \rightarrow \underline{k} + M_n - 1) \right\}$$

Kondo did not explain why a relaxation time should exist for this type of inelastic scattering. Equation (1.7) is the form of a trial function for electrical conduction in the variational method, so maybe it is a good approximation (Ziman 1960). In general a relaxation time can be defined if it is the same for both thermal and electrical processes. This is the case if the scattering is quasi-elastic (Blatt 1968).

This is usually true if $|E-E'| \ll kT$.

The scattering term for spin-flip scattering can be put into canonical form, for if

$$f - f^0 \equiv \phi \frac{\partial f^0}{\partial E} = \frac{1}{kT} f^0 (1-f^0) \phi$$

equation (1.6) becomes

$$\sum_{n\underline{k}'} W(\underline{k}' - M_n \rightarrow \underline{k} + M_n + 1) f^{0'} (1-f^0) (\phi' - \phi) = \frac{1}{kT} \sum_{n\underline{k}'} P(\underline{k}' - M_n \rightarrow \underline{k} + M_n + 1) (\phi' - \phi)$$

Doing this to all the terms yields

$$\left. \frac{\partial f}{\partial t} \right)_{\text{scatt.}} = \frac{1}{kT} \int P(\underline{k}, \underline{k}') (\phi - \phi') d\underline{k}'$$

where $P(\underline{k}, \underline{k}')$ is again the total equilibrium transition rate for all the processes.

The general transport coefficients involve electrical and thermal currents, \underline{j} and \underline{u} . Per unit volume they are

$$\underline{j} = -\int e \underline{v} f d\underline{k} \tag{1.8}$$

$$\underline{u} = \int \underline{v} (E - u) f d\underline{k} \tag{1.9}$$

u is the chemical potential or Gibbs free energy per electron, and f is the solution of the Boltzmann equation. Since the equilibrium distribution f^0 gives rise to no current, we can

replace f in the above equations by $f - f^0$. Where there is no temperature gradient, it is convenient to define

$$f - f^0 \equiv -e\underline{E} \cdot \underline{\Lambda}(\underline{k}) \frac{\partial f^0}{\partial E} \quad (1.10)$$

where $\underline{\Lambda}(\underline{k})$ is the so-called vector mean free path. The Boltzmann equation with a relaxation time becomes

$$\frac{f-f^0}{\tau} = -e\underline{v} \cdot \underline{E} \frac{\partial f^0}{\partial E} = -\frac{1}{\tau} e\underline{\Lambda} \cdot \underline{E} \frac{\partial f^0}{\partial E}$$

or

$$\tau \underline{v} = \underline{\Lambda} .$$

Putting equation (1.10) into (1.8)

$$\underline{u} = -\underline{E} \cdot e \int (E-u) \underline{v} \underline{\Lambda} \frac{\partial f^0}{\partial E} \equiv \underline{\phi} \cdot \underline{E} .$$

Now the relation between \underline{E} and \underline{j} is well known,

$$\underline{j} = \underline{\sigma} \cdot \underline{E} \quad \text{or} \quad \underline{E} = \underline{\sigma}^{-1} \cdot \underline{j}$$

where $\underline{\sigma}$ is the electrical conductivity tensor. Then

$$\underline{u} \equiv \underline{\Pi} \cdot \underline{j} = \underline{\phi} \cdot \underline{\sigma}^{-1} \cdot \underline{j}$$

or

$$\Pi = \underline{\phi} \cdot \underline{\sigma}^{-1} \quad (1.11)$$

is the Peltier coefficient of thermoelectricity.

From the Kelvin-Onsager relations, the thermopower, \underline{s} , is given by

$$\underline{\tilde{s}} = \text{(transpose of } \underline{s} \text{)} = \underline{\Pi}/T.$$

$\underline{\sigma}$ is easily found from equations (1.10) and (1.8).

$$\underline{\sigma} = e^2 \int \underline{v} \underline{A} \frac{\partial f^0}{\partial E} d\underline{k}$$

Where a relaxation time exists, and the metal is considered to be isotropic

$$s = - \frac{1}{eT} \frac{\int (E-u) \tau v^2 \frac{\partial f^0}{\partial E} d\underline{k}}{\int \tau v^2 \frac{\partial f^0}{\partial E} d\underline{k}}$$

Changing over to integration over energies,

$$s = - \frac{1}{eT} \left\{ \frac{\int \tau(E) (E-u) \rho(E) v^2 \frac{\partial f^0}{\partial E} dE}{\int \tau(E) \rho(E) v^2 \frac{\partial f^0}{\partial E} dE} \right\} = - \frac{1}{eT} \frac{\int (E-u) \sigma(E) dE}{\int \sigma(E) dE} \quad (1.12)$$

where $\rho(E) = \frac{1}{8\pi^3} \int \frac{ds}{|\partial E / \partial \underline{k}|}$ is the density of states. (Kittel 1966).

A physically satisfying way of obtaining an expression for the Peltier coefficient was discussed by Fritzsche (1971). If

the conductivity is written

$$\sigma(E) = \int \sigma(E) dE$$

then $\sigma(E)$ is the percentage of the conductivity in the energy range dE . If each electron contributes to the energy transfer as to the charge transfer then

$$\Pi(E) = -\frac{(E-u)}{e} \frac{\sigma(E)}{\sigma}$$

is the energy carried in the energy range dE per unit charge.

$$\int \Pi(E) dE = \Pi = ST = -\frac{1}{e} \int (E-u) \frac{\sigma(E)}{\sigma} dE$$

This agrees with equation (1.11). Thus Π has the simple physical interpretation as the average energy carried by conduction electrons per unit charge.

If $F = \tau(E)\rho(E)v^2$ in the numerator and denominator of equation (1.12) are expanded in a power series about u , then

$$S = \frac{\Pi^3}{3} \frac{k^2 T}{e} \left. \frac{\partial \ln \sigma(E)}{\partial E} \right)_{E=u} ; \quad kT/u \ll 1 \quad (1.13)$$

to first order in kT/u . The details are worked out in Mott and Jones (1936). It is valid at temperatures where the impurity resistance is larger than the thermal resistance and above the Debye temperature because it is based on the relaxation time

approximation. The Nordheim-Gorter rule can be derived from this equation if Matthiessen's rule holds.

$$\begin{aligned} S_{\alpha} \frac{\partial \ln \sigma}{\partial E} &= - \frac{\partial \ln \rho}{\partial E} = - \frac{1}{\rho} \left(\frac{\partial \rho_1}{\partial E} + \frac{\partial \rho_2}{\partial E} \right) \\ &= - \frac{1}{\rho} \left(\rho_1 \frac{\partial \ln \rho_1}{\partial E} + \rho_2 \frac{\partial \ln \rho_2}{\partial E} \right) \end{aligned}$$

or

$$S = \frac{1}{\rho} (\rho_1 S_1 + \rho_2 S_2).$$

I-2 The Connection Between Thermal Resistivity and Thermopower

From a variational procedure Kohler (1949) derived the following expression relating the thermopower and thermal resistances due to independent scattering mechanisms:

$$S = \frac{1}{\bar{W}} \sum_i W_i S_i \quad (1.14)$$

The physical basis of the variational procedure lies in the thermodynamics of irreversible processes. Expressions for entropy production due to scattering and fields are found to be equal. The distribution satisfying the Boltzmann equation is the one which maximizes the entropy production.

The theory starts with the canonical Boltzmann equation. A scattering operator is defined, and from it the entire variational procedure follows. A reasonable guess is made for the trial function ϕ previously defined. The violent behavior of $f - f^0$ was ironed out by factoring out $\partial f^0 / \partial E$ which is sharply peaked at the Fermi surface so that a good trial function is not hard to find.

Kohler used a trial function of the form

$$\phi = C(E) k_x = \sum_n N_n (E-u)^n k_x$$

and worked out expressions for the transport coefficients in terms of ratios of infinite determinants which converged rapidly. In particular, he found that $W_i S_i$ was proportional

to an integral containing the collision operator linearly. Thus if the different scattering mechanisms present in a metal can be added together, then

$$WS = W_1S_1 + W_2S_2 \quad (1.15)$$

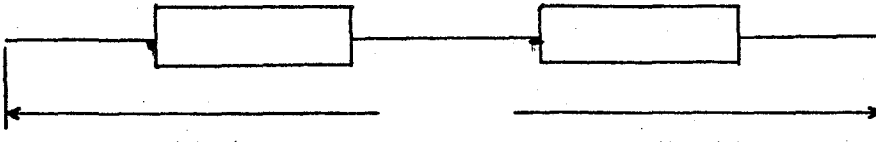
to a good approximation. The additivity of collision processes is possible if they don't occupy each other's intermediate or final states.

Matthiessen's rule is based on exactly the same reasoning as Kohler's rule as Kohler himself pointed out. The expression is not exact because the solution ϕ for a scattering operator $P=P_1+P_2$ is not necessarily the solution for P_1 and P_2 separately. Kohler showed that deviations from Matthiessen's rule should be small using the same variational procedures (Kohler 1949a). (Ziman 1960). One might say that equation (1.14) is the Matthiessen's rule of thermoelectricity.

In his derivation Kohler assumed that the lattice thermal conductivity is negligible compared to that of the electrons, and that the lattice is in thermal equilibrium, the Bloch assumption. As stated before this assumption is not valid when phonon drag components in the thermopower become important. He also assumed that alloying did not affect the density of conduction electrons.

Gold et al. (1960) have given a derivation of Kohler's rule which is intuitively appealing. If the different scattering mechanisms giving thermal and electrical resistance

in a metal can be treated as two conductors in a series with



$$\text{then } \Delta T_1 = \frac{W_1}{W_1+W_2} \Delta T \quad ; \quad \Delta T_2 = \frac{W_2}{W_1+W_2} \Delta T$$

$$V = S\Delta T = V_1+V_2 = S_1\Delta T_1 + S_2\Delta T_2 = \frac{1}{W}(W_1S_1+W_2S_2)\Delta T .$$

They justify this derivation with essentially the same assumptions as used by Kohler.

Since a relaxation time can be defined for elastic scattering that is the same for thermal and electrical currents, the Wiedemann-Franz law is valid.

$$L = \frac{\rho_i}{W_i T} .$$

Substituting into equation (1.14) one has the Nordheim-Gorter rule:

$$s = \frac{1}{\rho} \sum_i \rho_i S_i .$$

This was previously derived using equation (1.13) and Matthiessen's rule but with less generality since above Matthiessen's rule is not assumed.

The scattering of phonons at high temperatures is quasi-elastic so that the Nordheim-Gorter rule should hold for $T \gg \theta$. At low temperatures, $W_L \propto T^2$ and $\rho_L \propto T^5$ for the lattice phonon scattering. If the metal is pure enough so that at low temperatures, $T \ll \theta$, the lattice contribution to thermal and electrical resistivities dominates the impurity scattering, the Nordheim-Gorter rule should thus fail badly. In this case, Kohler's rule is much more useful. If sufficient impurities are present to dominate the scattering up to the Debye temperature, the Nordheim-Gorter rule should apply unless the impurity scattering is inelastic.

I-3 Kondo's Expression for the Thermopower of Dilute Magnetic Alloys

The nature of the scattering term in the Boltzmann equation for Kondo's treatment of the thermopower of dilute magnetic alloys has already been treated. Kondo worked out an explicit expression for the scattering probabilities using perturbation theory and the second Born approximation. For the unperturbed Hamiltonian he used

$$H_0 = \sum_{\underline{k}S} E(k) a_{\underline{k}S}^* a_{\underline{k}S} + 2\mu_B \sum_n \underline{H}_n \cdot \underline{S}_n$$

including the Zeeman energy of the n-th impurity atom feeling an effective field, \underline{H}_n , with spin of \underline{S}_n . The perturbing Hamiltonian included both a static perturbing potential, V, and the spin-spin exchange integral, J. From equation (1.12) one sees that only odd powers of energy will give non-vanishing contributions to the thermopower. The first term to do this is a J^3V term.

Kondo arrived at a first order expression for the thermopower of

$$S = \frac{R_{\text{mag}}}{R} F(T) \tag{1.16}$$

where $F(T)$ tends to a constant at high temperatures and to zero at low temperatures, $R_{\text{mag}} \propto J^2 S(S+1)$ and $R \propto V^2 + J^2 S(S+1)$.

R_{mag} is the resistivity due to the exchange energy alone, and R is the total resistivity due to the Fe. The $\ln T$ temperature

dependence of σ was neglected in the denominator of equation (1.12) as it is not so rapidly varying a function of T as the numerator. Also $\sigma(E)$ and $V(E)$ were replaced by their values at the Fermi surface. Qualitatively, equation (1.16) should hold when phonon and non-magnetic impurities are present if R is taken as the total resistivity, according to Kondo. Thus at low temperatures where the diffusion component of thermopower is small, equation (1.16) reduces to the Nordheim-Gorter rule.

The question may be asked as to how inelastic the above scattering is. In an earlier calculation, Kondo (1964) treated the case of magnetic spin-flip scattering neglecting the change in energy the impurity atom might undergo. That is, the unperturbed Hamiltonian was

$$H_0 = \sum_{\underline{k}} E(\underline{k}) a_{\underline{k} s}^* a_{\underline{k} s}$$

This means that the scattering was considered elastic. An extra resistivity proportional to $\ln T$ came out due to the fact that spin operators don't commute when considering intermediate states. It appears that in alloys where the Zeeman energies are small, ie. dilute alloys, the scattering can be considered quasi-elastic. The Wiedemann-Franz law should then be valid to a good approximation. Kohler's expression would reduce to the Nordheim-Gorter rule in this case.

Garbarino and Reynolds (1971) measured the thermal and electrical conductivities of dilute solutions of Fe in Au from 1K to 4.2K in temperature as shown in Figure 1.3. For dilute

enough alloys, $c \approx .027$ at .% Fe, the Lorentz ratio is constant, although about 4% higher than L_0 . At higher concentrations L flattens out at higher temperatures. This indicates that in the temperature range and Fe concentration of this experiment the scattering is quasi-elastic. Jha and Jericho (1971) performed similar measurements on $\underline{\text{Ag}}\text{-M}_n$ alloys and found similar results for the Lorentz ratio of these alloys.

I-4 Application of the Nordheim-Gorter Rule to Experiment

For two independent scattering processes the Nordheim-Gorter rule may be written as

$$\begin{aligned} S &= \frac{1}{\rho}(\rho_1 S_1 + \rho_2 S_2) = \frac{1}{\rho}(\rho_1 S_1 + [\rho - \rho_1] S_2) \\ &= S_2 + \frac{\rho_1}{\rho}(S_1 - S_2). \end{aligned} \quad (1.17)$$

If ρ_1 is held constant, by adding type 2 impurities a plot of S versus $1/\rho$ should yield a straight line whose intercept is the characteristic thermopower of that impurity in that solvent metal.

Deviations should occur whenever alloying distorts the Fermi surface or changes the density of conduction electrons, the scattering becomes significantly inelastic, or the Fermi surface is not approximately spherical. Kohler's expression is expected to be a much better relation when the scattering is inelastic, failing only when the lattice is not in thermal equilibrium.

The Nordheim-Gorter rule has been of great value in separating out the effects of trace impurities in "pure" metals. It points out that it is the relative, not the absolute, amount of impurities that determines which characteristic thermopower dominates. Gold et al. (1960) applied the rule to pure Cu with a number of impurity solutes. See Figure 1.4.

The plot for Fe is of special interest. Note the high value of the characteristic thermopower of Fe. The $1/\rho = 100$ point is for "pure" Cu put into a reducing atmosphere to remove any oxygen from impurities. The fact that this point fits on this plot indicates that this impurity is Fe. The straight line, however, depends strongly on this one point for its position.

MacDonald et al. (1962) have applied the rule to pure Au with Sn and Cu impurities. See Figure 1.5. Note that Cu and Sn are both non-magnetic and have approximately the same very small characteristic thermopower. The high value of about $4\mu\text{V}/\text{K}$ for pure Au is probably due to Fe impurities.

Blatt and Lucke (1967) made an interesting extension of the applicability of the Nordheim-Gorter rule. They noted that the thermopowers of Cu with Ga, Ge, and As solutes obeyed the rule even when deviations from Matthiessen's rule were quite severe. See Figures 1.6 and 1.7. They were able to extend the expected validity of the rule to cases where the alloy obeyed the Bloch-Gruneisen approximation for the total resistivity less the residual resistivity but with a different Debye temperature from the pure metal. ρ_1/ρ is replaced by ρ_1^A/ρ where $\rho_1^A = \rho_1 \frac{\theta_0}{\theta_A}^2$. A denotes the values for the alloy. When alloying distorts the Fermi surface severely, the rule is still expected to fail.

I-5 The Effect of Phonon Drag

Phonon drag is a result of coupling between electrons and phonons. An applied temperature gradient will cause the lattice to be in thermal disequilibrium. If there is a transfer of momentum to the conduction electrons, the thermopower can be considerably enhanced. In the steady state this transfer of momentum is balanced by an opposing electric field. This leads to an expression of the form (MacDonald 1962a)

$$S_g = \frac{1}{3Ne} C_g \quad (1.18)$$

where S_g is the thermopower due to phonon drag, N is the density of conduction electrons and C_g is the lattice specific heat per unit volume.

Equation (1.18) was derived assuming that electrons do all the phonon scattering. In reality phonons scatter off lattice defects, impurities and other phonons. To take this into account, MacDonald (1962a) made the following approximation:

$$S_g \cong \frac{C_g}{3Ne} \frac{\tau_p}{\tau_p + \tau_{pe}} = \frac{K}{e} \frac{\tau_p}{\tau_p + \tau_{pe}}$$

where τ_{pe} is the phonon-electron relaxation time and τ_p is the phonon relaxation time due to all other processes. If τ_{pi} decreases inversely with impurity concentration, a reasonable assumption for small amounts of impurity, then since ρ_1 increases linearly with impurity concentration

$$1/\tau_{pi} = A_{pi} = C\rho_i$$

$$S_g = \frac{K}{e} \frac{\tau_p}{\tau_p + \tau_{pe}} = \frac{K}{e} \frac{A_{pe}}{A_p + A_{pe}}$$

where A's are the transition probabilities

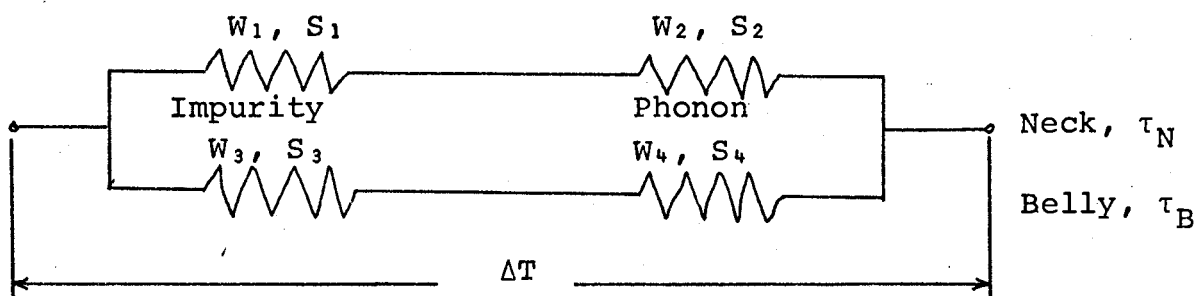
$$\frac{K}{e} \frac{A_{pe}}{A_{pp} + A_{pi} + A_{pe}} = \frac{K}{e} \frac{A_{pe}}{A_{pp} + A_{pe}} \frac{A_{pp} + A_{pe}}{A_{pi} + A_{pp} + A_{pe}} \cong S_g^0 \frac{A^0}{C\rho_i + A^0}$$

where A^0 and S_g^0 are the phonon transition probability and phonon drag thermopower respectively before the addition of impurities. Thus phonon drag might be expected to decrease in magnitude with increasing impurity concentration.

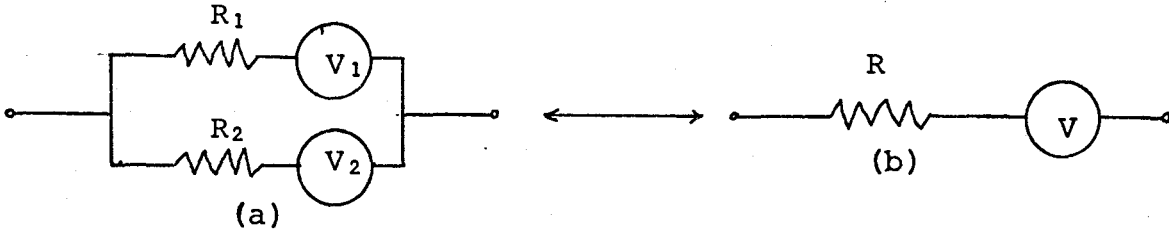
I-6 The Effect of Anisotropy on the Validity of the Nordheim-Gorter Rule

For spherical Fermi surfaces and elastic scattering the Boltzmann equation has an exact solution for thermal processes with the trial function $\phi = (E-u)\underline{k} \cdot \underline{n}$ where \underline{n} is a unit vector parallel to the applied external gradient. Since it is an exact solution regardless of the particular scattering mechanism, Kohler's law should hold exactly. Since the variational procedure is not particularly sensitive to the form of the trial function, Kohler's rule should still be a good approximation when the conditions for an exact solution are not met.

To take into account the known anisotropic Fermi surface of Au, Guenault (1972) has suggested a two band model with anisotropic relaxation times. Dugdale and Basinski (1967) accounted for deviations in Matthiessen's rule in dilute Cu and Ag alloys using the same model. One band consists of the "belly" electrons while the other consists of the "neck" electrons. These two independent groups of electrons have different scattering relaxation times for different processes. Guenault appealed to an equivalent circuit analogy after that of Gold et al. (1960).



If the thermal gradient is proportioned out to the impurities in each leg as $[W_1/(W_1+W_2)]\Delta T = \Delta T_1$ where W is the thermal resistivity, then $V_1 = S_1 T_1$ is the voltage developed. By the ladder theorem of electrical circuit theory the circuit (a) is equivalent to circuit (b) where



$$V = (V_1/R_1 + V_2/R_2) / \left(\frac{1}{R_1} + \frac{1}{R_2} \right)$$

Applying this to the above thermal circuit and further assuming that the scattering is elastic so that the thermal resistivities may be replaced by the electrical resistivities,

$$S = \frac{(R_1 S_1 + R_2 S_2) / (R_1 + R_2)^2 + (R_3 S_3 + R_4 S_4) / (R_3 + R_4)^2}{1 / (R_1 + R_2) + 1 / (R_3 + R_4)} \quad (1.19)$$

At low temperature the phonon contribution is negligible, $(W_2, W_4 \leq W_1, W_3)$ and this reduces to

$$S_0 = (S_1/R_1 + S_3/R_3) / (1/R_1 + 1/R_3)$$

In the isotropic case τ_N/τ_B is the same for impurity and phonon scattering and thus $\frac{R_1}{R_3} = \frac{R_2}{R_4}$. (The center of the equivalent circuit can be shorted.) Then equation (1.19)

reduces to the Nordheim-Gorter rule. For dilute alloys at high temperatures where $R_1 \ll R_2$ and $R_3 \ll R_4$, one gets with some algebra

$$S = \frac{1}{\rho_L + \rho_O} (S_L \rho_L + S_O^1 \rho_O)$$

except that S_O^1 is no longer the characteristic thermopower of the impurity. S_O^1 depends on S_O , S_2 , S_4 and τ_N/τ_B . That is, a plot of S versus $1/\rho$ will give a straight line but with a different interpretation from the Nordheim-Gorter rule. For concentrated alloys, the Nordheim-Gorter plot will be curved.

With so many parameters available one can, of course, come to agreement with a great variety of data. Guenault treats Ag alloys where Fe contamination is less of a problem than with other noble host metals. He measured the thermopower of various alloys at very low temperatures and fitted an equation of the form

$$S(T) = AT + BT^3 + CT/(T + T_O)$$

to experimental data for diffusion, phonon drag and Kondo thermopower respectively. He found that C was very small and deduced from A the characteristic thermopower of various impurities in Ag. He then compared these values with those from intercepts of Nordheim-Gorter plots from other sources.

For Ag-In and Ag-Tl there was agreement; for Ag-Au and

Ag-Ge the Nordheim-Gorter plots gave about twice the value. That is, the experimental evidence is scarce and inconclusive for this problem. Furthermore, for very concentrated Ag-Au alloys, refer to Figure 1.9, the Nordheim-Gorter rule hangs on for much longer than the two band model which experimentally determined parameters predict. The two band model does, however, make interpretation of the intercept of a Nordheim-Gorter plot open to question.

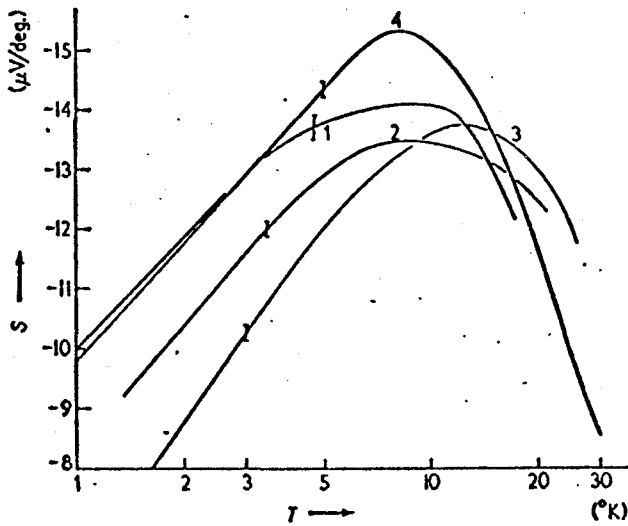


Figure 1 Absolute thermopower of several dilute gold-iron alloys. Vertical lines represent typical uncertainties.

- 1: 99.99 per cent pure Au + 0.02 per cent (at.) Fe
- 2: 99.97 per cent pure Au + 0.035 per cent (at.) Fe
- 3: 99.995 per cent pure Au + 0.06 per cent (at.) Fe
- 4: Spec. pure Au + 0.03 per cent (at.) Fe

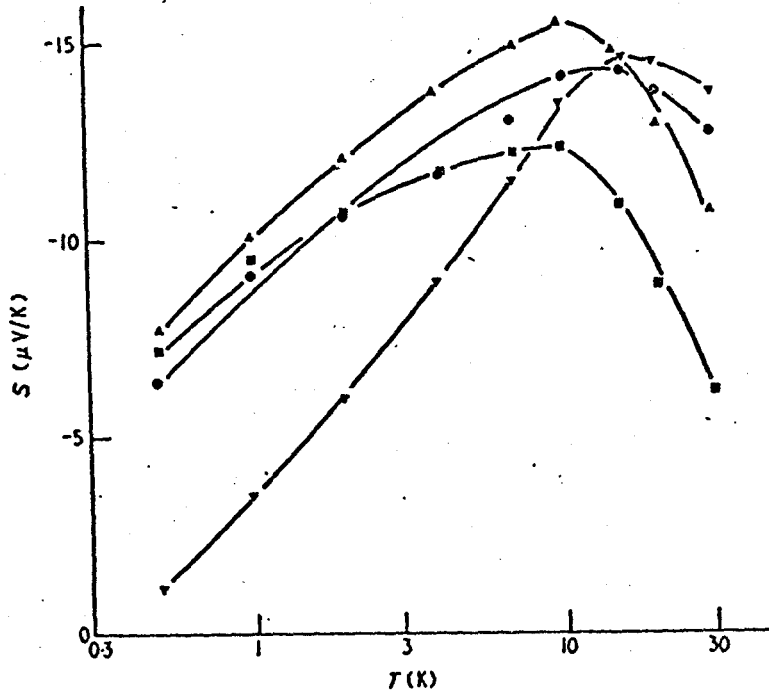


Figure 1.2 The thermoelectric power of Au-Fe alloys for various Fe concentrations. \blacksquare 110 ppm; \blacktriangle 300 ppm; \bullet 1100 ppm; \blacktriangledown 1900 ppm.

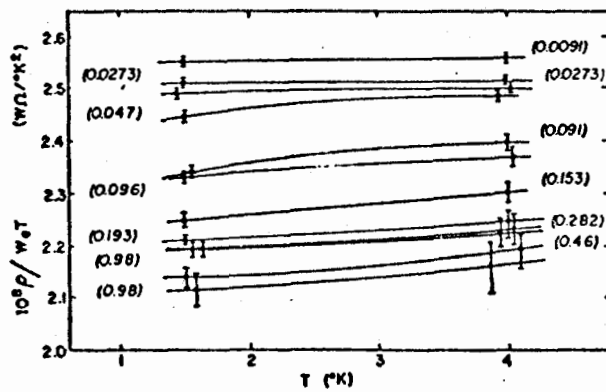


Figure 1.3 Lorenz ratio plotted against temperature.

Numbers in parentheses refer to the impurity concentration of the sample at at. %. Error bars indicate the uncertainty in temperature variation, due mainly to the fractional size of the lattice conductivity.

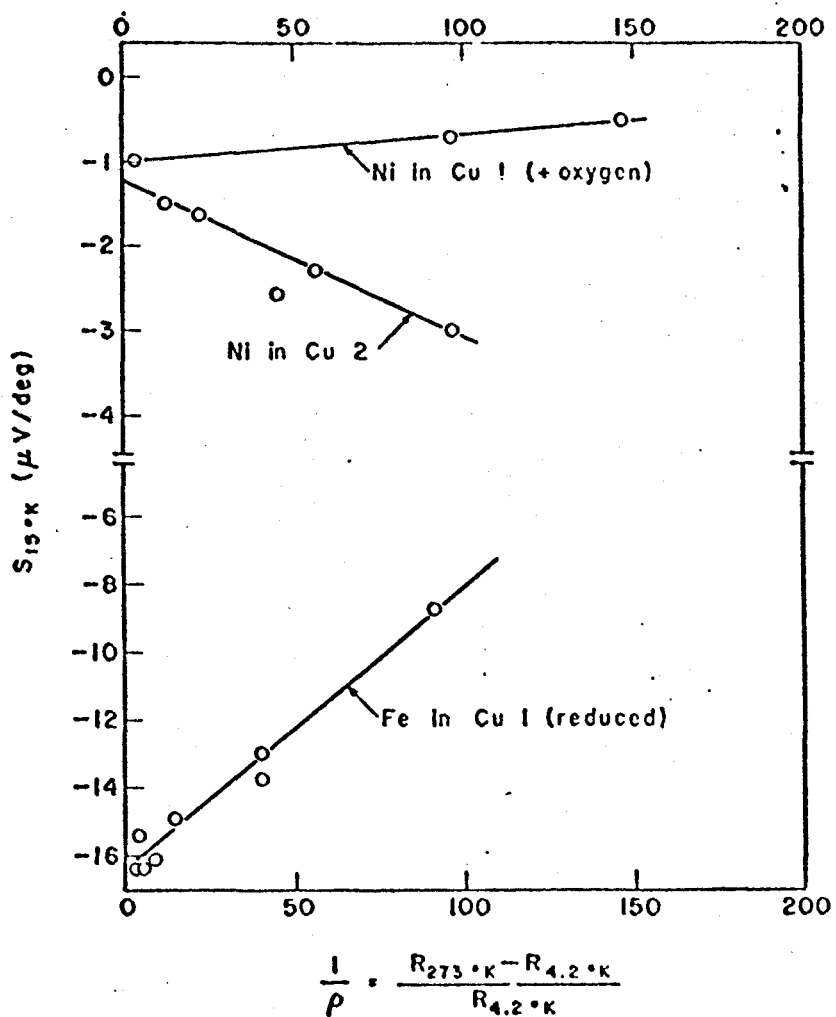


Figure 1.4 Nordheim-Gorter plot of various dilute alloys of copper

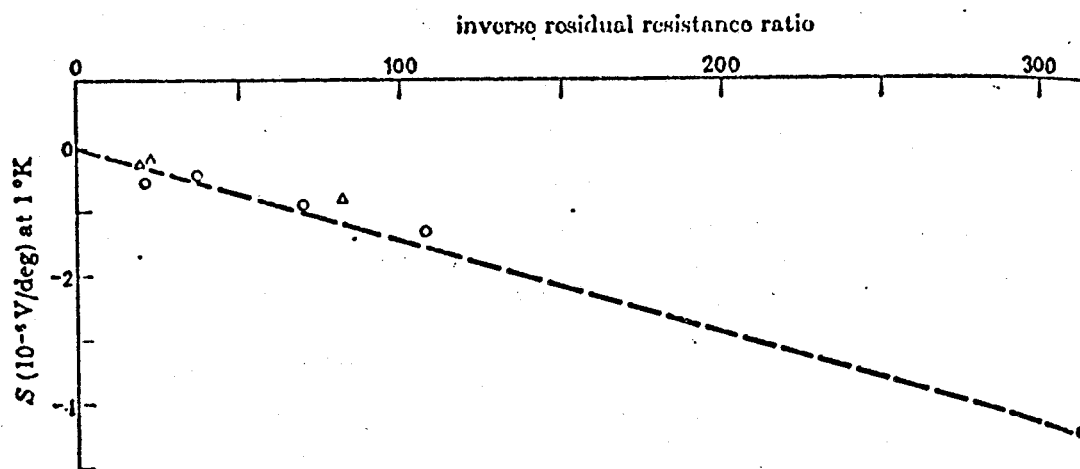


Figure 1.5 Absolute thermo-electric power (S) of dilute Au + Sn Alloys at 1°K as a function of inverse residual resistance ratio.

The experimental point marked with a solid circle indicates the nominally 'pure' starting specimen of gold. Plotting thermo-electric power in this way (the 'Nordheim-Gorter rule'—cf. for example, Gold *et al.* 1960) enables one to determine readily the *characteristic* thermo-electric power due to a given solute. The intercept on the ordinate when the abscissa tends to zero should give this characteristic thermo-electric power and with Cu and Sn as solutes it is clear that this is very small at 1°K ($S \rightarrow 0$ approx. as the abscissa tends to zero).

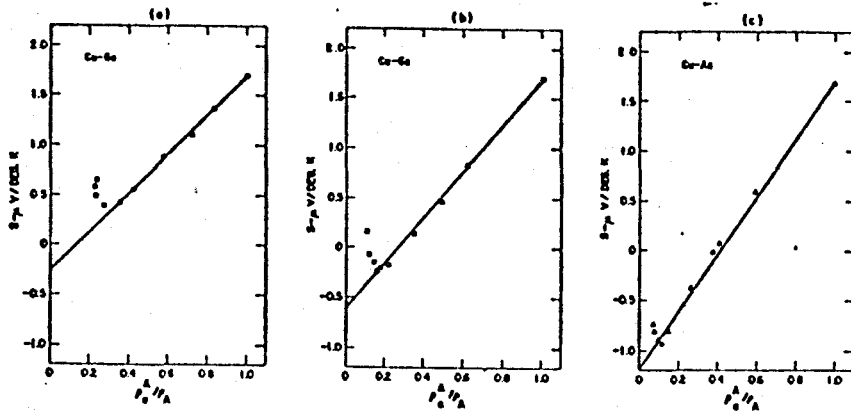


Figure 1.6

Modified Gorter-Nordheim plots at 290°K for solid solutions of (a) gallium, (b) germanium, and (c) arsenic in copper.

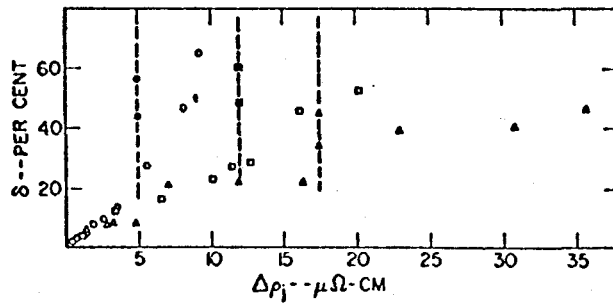


Figure 1.7

Per cent deviation from Matthiessen's rule at 290°K as a function of residual resistivity for Cu-Ga —○—, Cu-Ge —□—, and Cu-As —△— alloys. (After Crisp *et al.* 1964.)

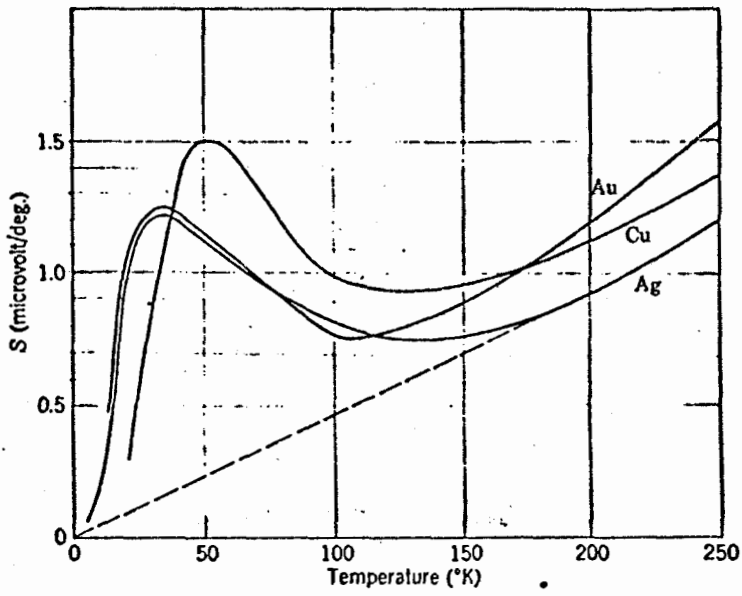


Figure 1.8 Absolute thermopower of some pure noble metals.

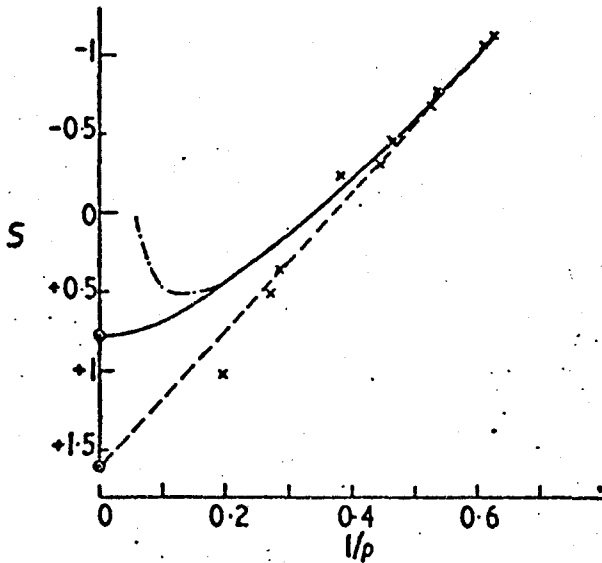


Figure 1.9 Nordheim-Gorter plots for dilute Ag alloys at 300 K.

Full curve, theoretical, calculated from equation (3) using parameters proposed for AgAu (see text); x data of Crisp and Rungis (1970) for AgAu; chain curve, schematic form of graph obtained for a heterovalent Ag alloy (data of Köster and Rave (1964), after Foiles (1970)); o indicate values of x_0 and x_0^{NGR} (see text).

CHAPTER II

EXPERIMENTAL

II-1 Sample Preparation

All the Au-Fe-Sn alloys were made from Johnson Matthey thermocouple wire .08 mm in diameter with nominal 0.03 at % Fe concentration. The residual resistance ratio, $R_{4.2}/R_{295-R_{4.2}}$ was .145 corresponding to about 360 ppm Fe using data from the literature (MacDonald 1962). The varnish coating was removed with Strip-X, a commercially available product. Concentrated formic acid was easier to use but left behind a slight residue.

About 30 cm of the above wire was coiled and suspended about 10 cm above the Ta boat of a small evaporator. Small amounts of pure Sn were evaporated onto the Au-Fe alloy at a pressure of about 4×10^{-4} Torr. The wire was placed in a small quartz glass tube, 7 cm x 1 cm, pumped down to 10^{-5} or 10^{-6} Torr, and sealed off. The tube was then placed in an electric oven at 850C for 24 hours. Au melts at 1063C.

The Sn disappeared from the surface sometime before the oven reached full temperature, so 24 hours was deemed enough time to give uniform distribution of the Sn throughout the Au. A more rigorous argument using the diffusion equation is given in Appendix I. The oven was turned off with the specimen tube still inside and left to cool down for an anneal.

The residual resistance ratio was measured by mechanically

clamping about 5 cm of the sample into a simple four probe dip cryostat. A wrapping of teflon tape provided most of the pressure. To check for uniformity, one sample was measured in 5 cm segments along its entire 30 cm length and found to be uniform to about one percent.

The approximate Sn concentration was found using data of MacDonald et al. (1962) who found that the increase in residual resistance ratio due to Sn in Au was 1.365 per at.%. If the increase in resistivity is due entirely to Sn, and Matthiessen's rule is obeyed, the Sn concentration can be calculated. The results of the above sample preparation are summarized in Table 1. A justification of Matthiessen's rule is given in Appendix II. Sample VI was the highest concentration attempted since the solubility of Sn in Au is about 0.2 at.% at 200 C (Hansen 1958).

The samples were submitted to Cantest Limited for a quantitative flame spectrographic analysis. This firm overestimated its equipment's resolving power and was unable to detect the Sn in such small samples.

TABLE 1

Residual Resistance and Approximate Sn
Concentrations of the Au-Fe-Sn Specimens

Sample	$r = R_{4.2} / (R_{295} - R_{4.2})$	Δr	Sn conc. (ppm)
I	.148	0	0
II	.177	.029	212
III	.188	.040	293
IV	.231	.083	608
V	.404	.256	1875
VI	.828	.680	4980

II-2 Thermopower Measurement

The cryostat used for the present experiments is shown in Figure 2.1. It was inserted through an O-ring seal into a wide neck He dewar for the temperature range 4.2 to 77K and into LN₂ for higher temperatures. The temperature was varied by changing position relative to the liquid level and applying small amounts of heat to the upper block. About 2 mm pressure of He exchange gas was used.

The Au+.03 at .% Fe versus chromel thermocouple used to measure temperature was calibrated to 100K against a Germanium resistance thermometer with factory calibration.

That is

$$V = \int_T^{273.2} (S_{\text{chromel}} - S_{\text{Au-Fe}}) dT$$

was measured using the resistance thermometer to obtain T. The thermocouple was used for determining temperatures instead of the resistance thermometer because it is easier to use, cheaper, and less fragile. Its disadvantages will be mentioned later.

Temperature versus voltage tables were obtained by fitting parabolas to successive small segments of the raw data. The values obtained differed somewhat from other sources, indicating that at the present state of quality control among manufacturers, it is necessary to calibrate Au-Fe thermocouples

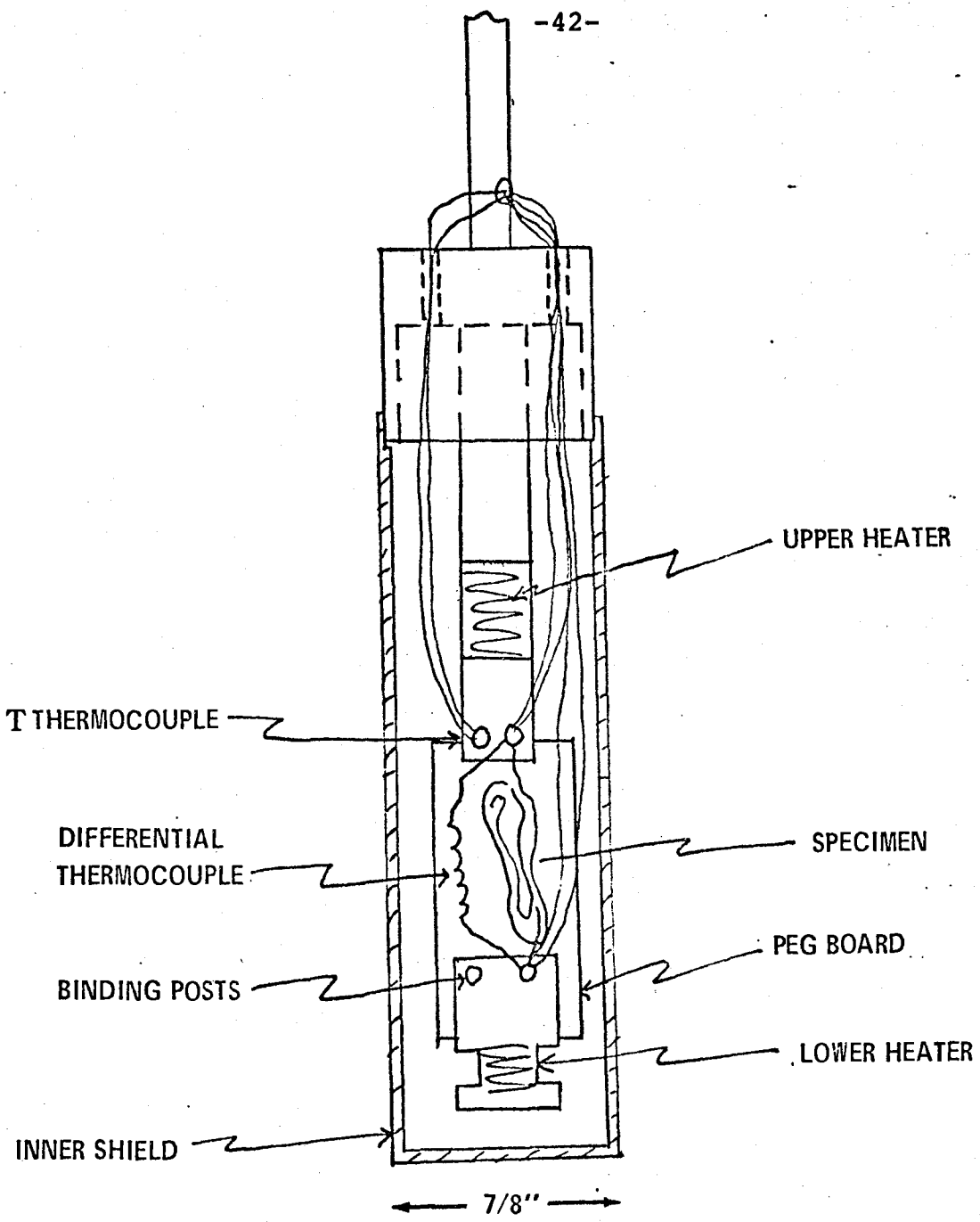


Figure 2.1 Lower Portion of apparatus

yourself. The present Au-Fe thermocouple wire was obtained from Johnson Matthey, the same wire used to make the Au-Fe-Sn alloys.

By differentiating the small parabolic segments of the voltage versus temperature graphs, $(S_{\text{chromel}} - S_{\text{Au-Fe}})$ was determined. To measure the temperature gradient between the upper and lower blocks of the cryostat, a differential thermocouple was made from the same wire. Then

$$V(\Delta T) = \int_T^{T+\Delta T} (S_{\text{chromel}} - S_{\text{Au-Fe}}) dT \cong (S_{\text{chromel}} - S_{\text{Au-Fe}}) \Delta T$$

gives a direct reading of the temperature gradient if ΔT is sufficiently small.

The samples whose thermopower was to be measured were encased in teflon spaghetti and folded into small bundles. About 5 cm on each end was wrapped onto the binding posts of the cryostat over cigarette paper and glued with GE 7031 varnish for a thermal bond. The differential voltages were read directly off a Keithley 148 nanovoltmeter, an oil immersed low thermal switch changing from the specimen to the differential thermocouple.

The difference in thermopower between the untreated and alloyed Au-Fe was measured directly using untreated Au-Fe leads up to the voltmeter. The absolute thermopower of the untreated Au-Fe was determined using 99.9999% pure Pb as a sample. The absolute scale of Christian et al. (1958) for

Pb was subtracted from this data, giving $S_{\text{Au-Fe}}$. The Pb wire used was relatively thick, .25 mm in diameter, and a fair length, 90 cm, was found necessary to reduce its thermal conduction. When the sample has a thermal conductivity on the order of the thermal contacts through the cigarette paper, the temperature gradients are considerable.

Since the thermopower of the untreated Au-Fe was used as a reference for all the differential measurements of $S_{\text{Au-Fe}}$ - $S_{\text{Au-Fe-Sn}}$, it was necessary to know its value with confidence. The specimen leads up to the cryostat were changed from Au-Fe to Pb and a specimen of chromel was mounted into the cryostat. From this S_{chromel} was determined which can be combined with the data from the differential thermocouple calibration to give an alternate determination of $S_{\text{Au-Fe}}$.

Two different temperature gradients were set up between the upper and lower blocks for each differential measurement. The two voltages obtained were subtracted to obtain $V(\Delta T)$ and the specimen voltage, V_S . $V(\Delta T)$ was typically 25μ V. This was done to lessen the effect of thermals. That is, when $V(\Delta T) = 0$, $V_S \neq 0$. If large temperature gradients are used, the effect is negligible, but large gradients mean fast temperature drifts if no external heat is supplied. Too much external heat would cause the temperature of the temperature-sensing thermocouple to be different from that at the specimen, a fact noted when calibrating the thermocouple against the Ge resistance thermometer.

As it turned out, it was difficult to keep the temperature constant for two different differential readings, so that the two methods are probably equivalent in usefulness, at least in this cryostat. If the exchange gas were pumped out, the temperature drifts would slow down. It was thought that if some of the temperature gradient was maintained through the exchange gas, it would lessen the errors due to heat conduction through the sample.

The main sources of experimental error were due to the alloying procedure and the apparatus. It was hoped that adding Sn to the Au-Fe would do nothing to any oxidized Fe in the wire. When the plated Au-Fe wire was removed from the evaporator, surely some of the Sn oxidized. For the most dilute alloys, perhaps 20% of the Sn was oxidized if oxidation occurred for a couple of monolayers. SnO probably has a different characteristic thermopower from Sn. It may have helped to have subjected all the samples to a reduction process such as heat treatment with H₂ or Co. It is also to be noted that annealing increased the residual resistance of the unplated Au-Fe. Whether this is due to reducing Fe oxides, redistributing the Fe, or just inhomogeneous wire is unknown.

As for the apparatus, the main errors come from thermals. If the Au-Fe or chromel wires were not uniform along their length, different thermal environments would give changing voltage readings. That is,

$$V = \int_T^{273.2} \Delta S(\underline{r}, T(\underline{r})) dT = \int_T^{273.2} \Delta S(\underline{r}, T(\underline{r})) \frac{\partial T}{\partial \underline{r}} d\underline{r}$$

would no longer be independent of the temperature distribution. That this was the case with this thermocouple was certified when upon pulling the cryostat up slightly from the He bath, the apparent temperature went down. A possible error $\pm 2\text{K}$ could have arisen in this way. For the $V(\Delta T)$ measurement similar thermals could occur due to slow drifts, but the subtraction of voltages should have minimized this.

It was also found that $V(4.2\text{K})$ varied slightly from experiment to experiment, although never more than half a percent. The ratio $V(4.2 \text{ observed})/V(4.2 \text{ tables})$ was used to calculate the temperature in this case.

As mentioned earlier, the cigarette paper and GE varnish is not a perfect thermal contact. The only time it gave real trouble was when pure Pb was used as a specimen where it was found necessary to use 90 cm. The thermal conductivity of Au-Fe is appreciable, and could have affected the results in an unknown way, giving persistent errors in the thermopower determination. However, one Au-Fe-Sn specimen was mounted twice giving the same results for the thermopower.

CHAPTER III

EXPERIMENTAL RESULTS

III-1 The Thermopower of Au-Fe-Sn Alloys

The thermopower of the untreated Au-Fe alloy was determined in two independent ways. It was measured directly against Pb. The thermopower of chromel was also measured against Pb and then subtracted from the tables of $(S_{\text{chromel}} - S_{\text{Au-Fe}})$ constructed for the differential thermocouple. This gives a check on the other data. The two sets of data were combined and smoothed out with a least squares parabolic fit of small segments of data. The parabolic constants were used to calculate a table of $S_{\text{Au-Fe}}$ versus temperature.

The measured values of $(S_{\text{Au-Fe}} - S_{\text{Au-Fe-Sn}})$ were subtracted from this table and plotted directly. A french curve was used to draw in a smooth interpolation. The results are shown in Figure 3.1. The thermopower of the most concentrated alloys was obtained from subtracting two numbers of equal magnitude and exhibit the most scatter. One sees that the effect of adding Sn is to reduce the thermopower.

III-2 The Resistivity of Au-Fe-Sn Alloys

Although the residual resistance ratio of the Au-Fe-Sn alloys at 4.2K and 295K was measured, the resistivity as a function of temperature was not. The question is whether one can add this on unabashedly to the ideal resistivity at other temperatures. That is, how valid is Matthiessen's rule for this particular ternary alloy. Since the literature does not abound with discussions of the resistivity of ternary alloys, it is here assumed that deviations will not exceed those typical for binary alloys. Then

$$\frac{\rho(T)}{\rho_L(295)} \cong \frac{\rho_L(T)}{\rho_L(295)} + \frac{\rho(4.2)}{\rho(295) - \rho(4.2)} \cong \frac{\rho_L(T)}{\rho_L(295)} + r$$

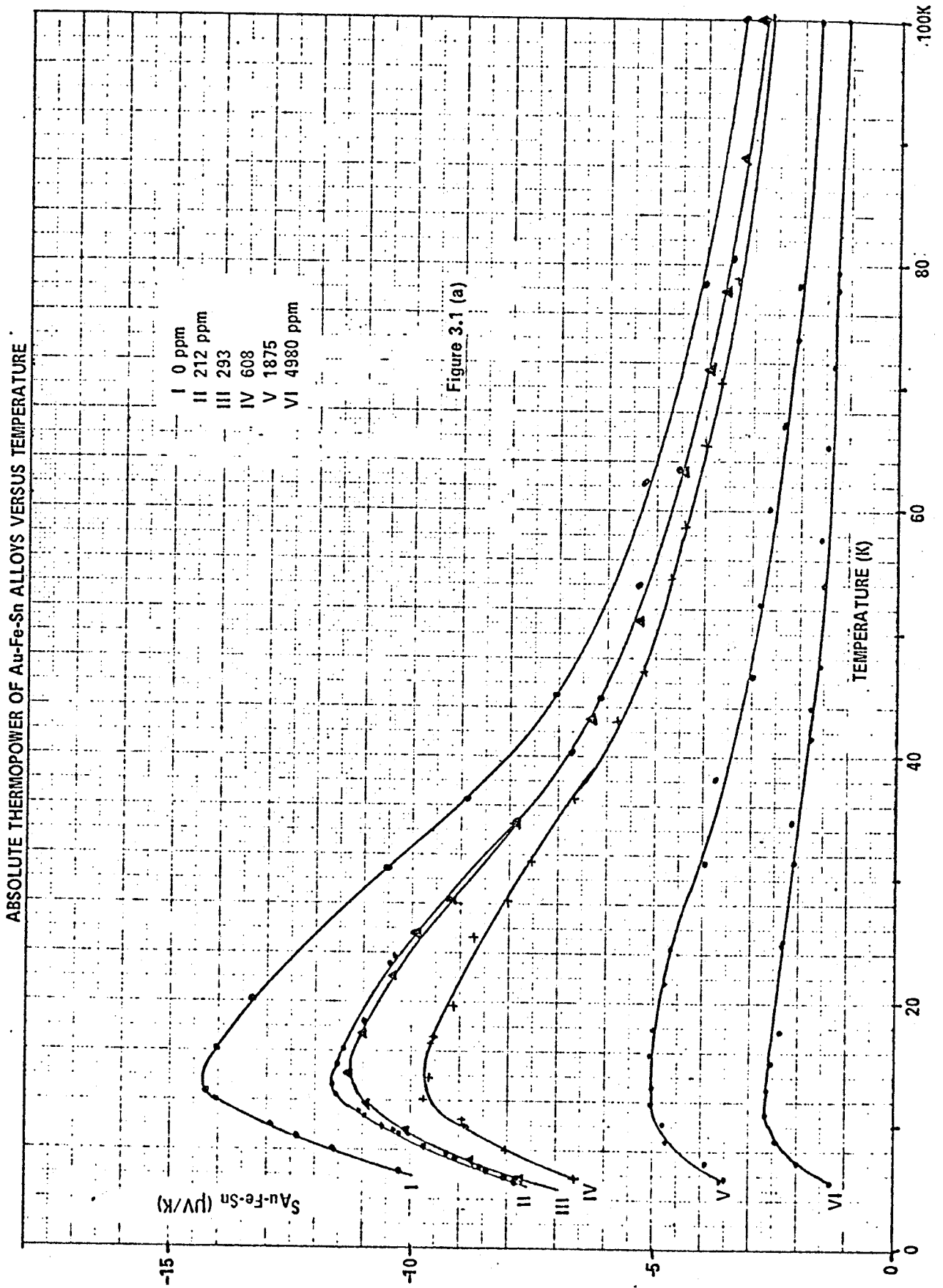
Refer to Appendix II for a discussion of the validity of this procedure. ρ_L is the ideal lattice resistivity.

III-3 The Nordheim-Gorter Plots

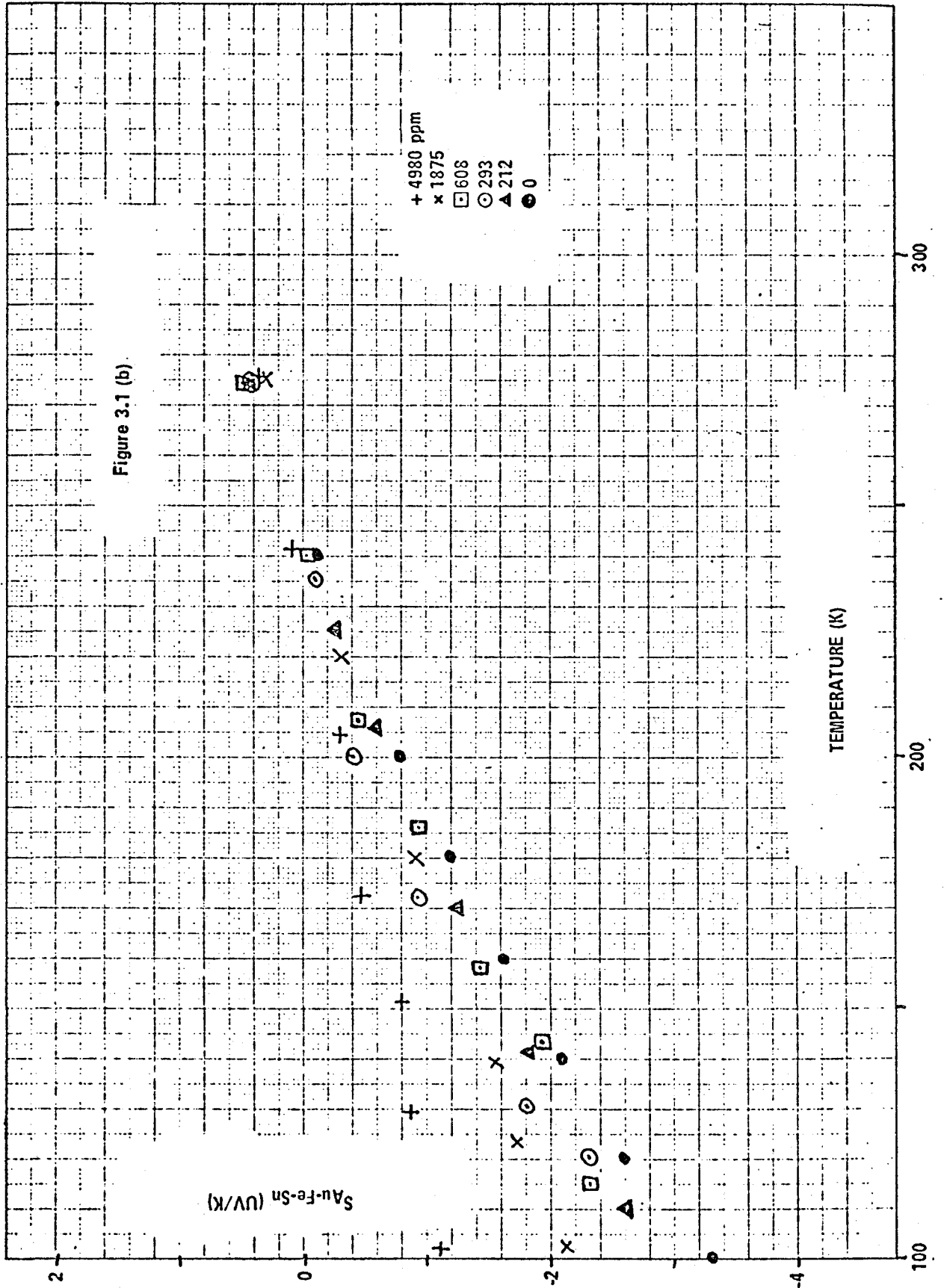
Combining the results from the previous sections the measured absolute thermopower can be plotted versus $\rho_L(295)/\rho(T)$. The thermopower was read directly off Figure 3.1. $\rho(T) = \rho(4.2) + \rho_L(T)$ by assumption. Temperatures ranged from 6K to 100K. See Figures 3.2, 3.3, and 3.4.

Error bars for uncertainty in resistance were determined from an estimated 5% possible deviation from Matthiessen's rule. Since deviations from this rule are invariably positive, the error bars lie to the left of all the points. Above 100K the range of $1/\rho$ is small and the plots are too scattered to be of any useful interpretation.

It is evident that the plots are all best fit by straight lines. At lower temperatures the range of $1/\rho$ is much larger, making for a more compelling fit. What scatter is present is most likely due predominantly to alloying problems or a different persistent error for each alloy, as the experimental points are consistently over or under the straight line fit. An example of a persistent error would be poor mounting of a specimen so that the temperature gradient across the specimen would be different from that across the differential thermocouple. An alloying problem would be the presence of oxygen in the quartz tube affecting the Fe.



ABSOLUTE THERMOPOWER OF Au-Fe-Sn ALLOYS VERSUS TEMPERATURE



LOW TEMPERATURE NORDHEIM-GORTER PLOTS FOR Au-Fe-Sn ALLOYS

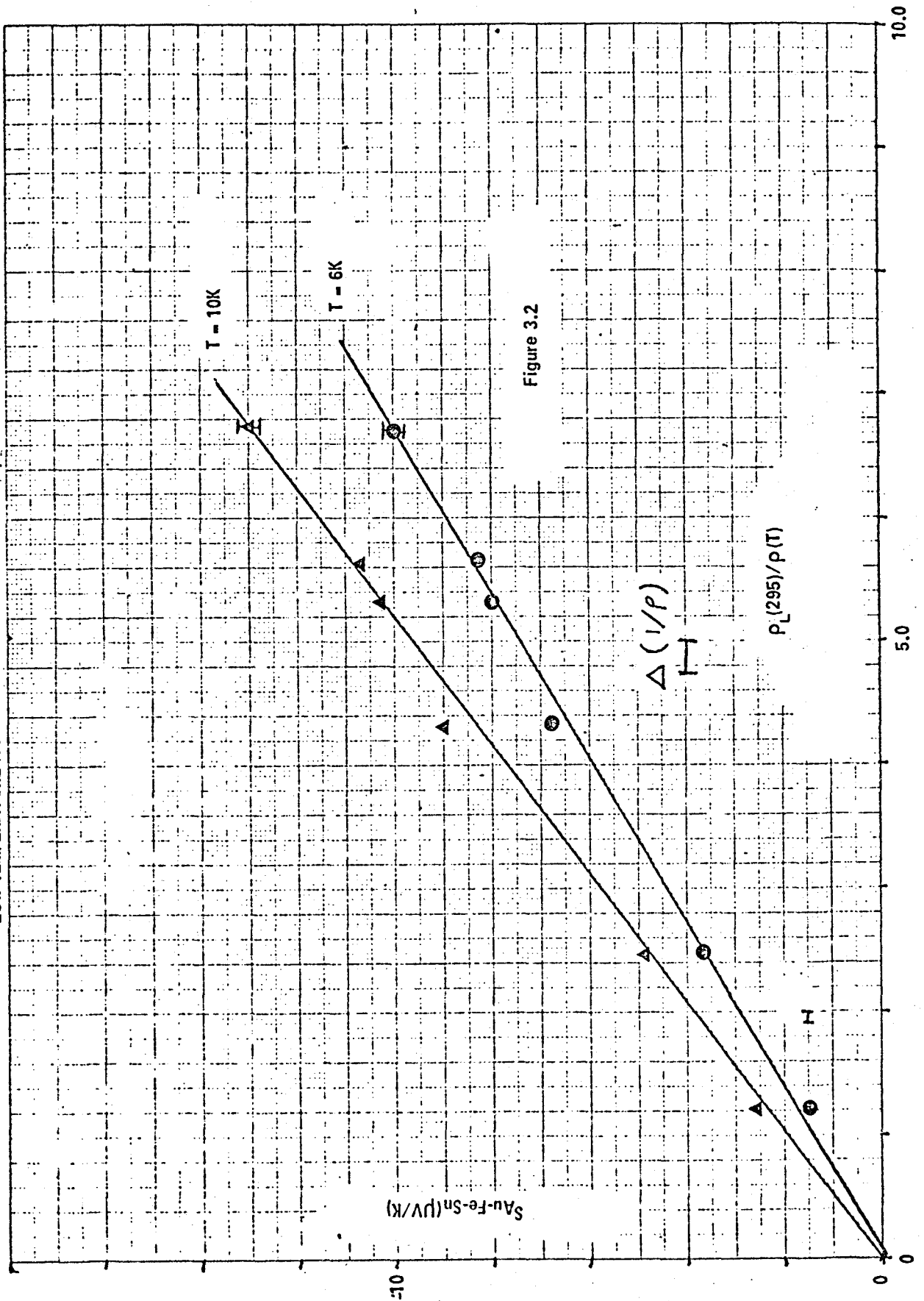


Figure 3.2

NORDHEIM-GORTER PLOT OF Au-Fe-Sn ALLOYS AT 25K

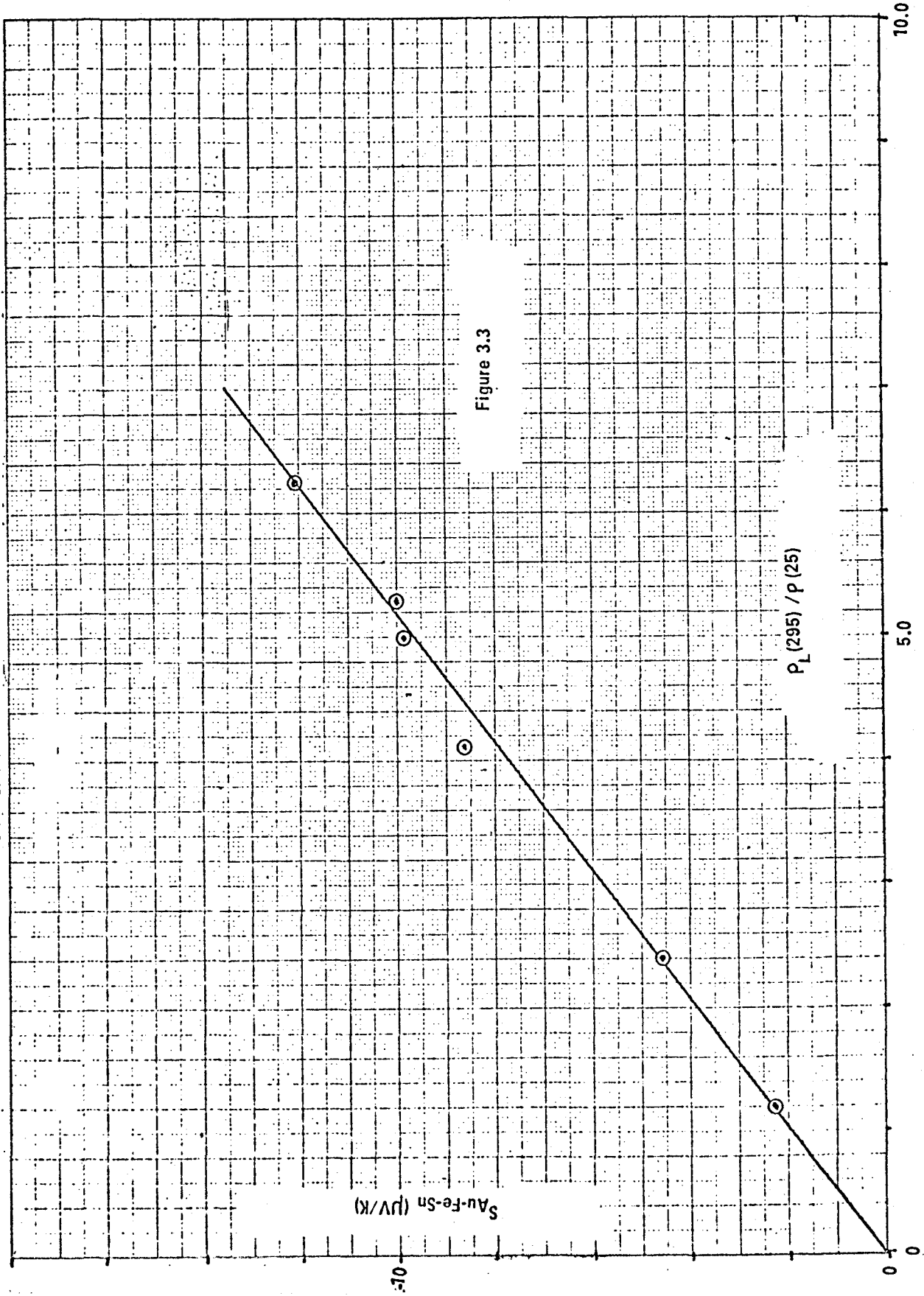
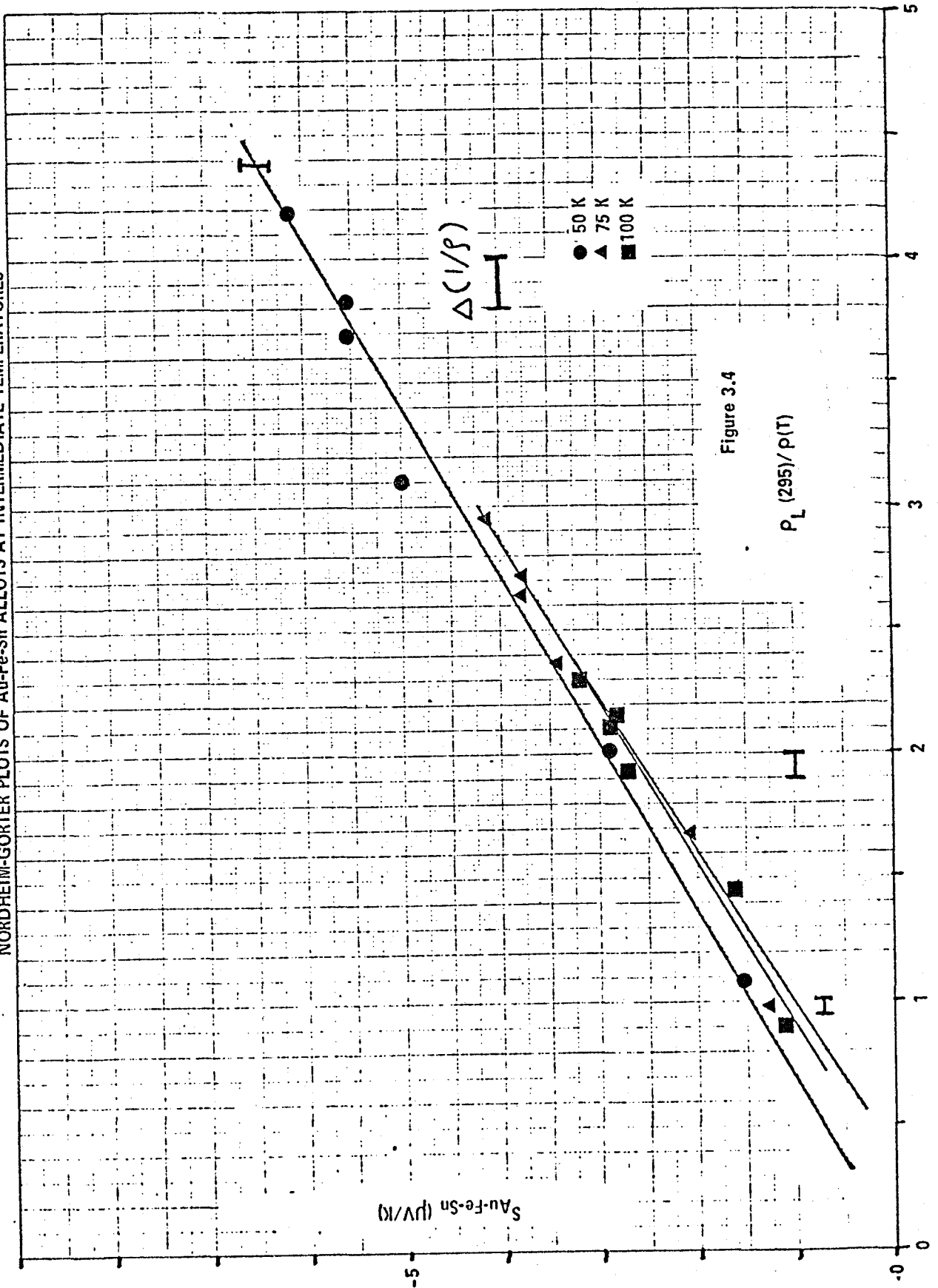


Figure 3.3

NORDHEIM-GORTER PLOTS OF Au-Fe-Sn ALLOYS AT INTERMEDIATE TEMPERATURES



CHAPTER IV

DISCUSSION AND CONCLUSIONS

In the temperature range 6K to 100K the Nordheim-Gorter rule provides a good explanation for the effect of Sn impurities on the thermopower of Au+0.03 at .% Fe even though the conditions for its validity are not strictly observed. At low temperatures it is the Fe which is responsible for almost all of the thermopower, so it is evident that the scattering of Fe impurities in this range of Fe concentration and temperature is predominantly elastic. This is in agreement with measurements of the Lorentz ratio, $L = \rho/WT$, performed by Garbarino and Reynolds (1971) for Au-Fe alloys of this concentration from 1K to 4.2K.

At higher temperatures phonon drag and inelastic phonon scattering are expected to cause deviations from the rule. Some measure of the relative contributions expected from inelastic (phonons) and quasi-elastic (impurity) scattering is to compare the electrical resistivities. At around 65K for the most dilute alloys up to 250K for the most concentrated alloy, the ideal resistivity is equal to the residual resistivity.

Thus for the more concentrated alloys, the ones on the left of the Nordheim-Gorter plots, the total scattering of the electrons is predominantly elastic up to 100K. The high value of $S_{\text{Au-Fe}}(100\text{K}) = -3.2\mu\text{V/K}$ where $\rho_L \cong 2\rho_{\text{Fe}}$, indicates the Fe is still contributing significantly to the thermopower at this

temperature. For pure Au $S_L = 0.8 \mu\text{V/K}$ referring to Figure 1.8. Thus using Kohler's rule which is of greater value for inelastic scattering,

$$WS = W_{\text{Fe}} S_{\text{Fe}} + W_L S_L + W_{\text{Sn}} S_{\text{Sn}}$$

$$\frac{\rho S}{L} = \frac{\rho_{\text{Fe}}}{L_{\text{Fe}}} S_{\text{Fe}} + \frac{\rho_L S_L}{L_L} + \frac{\rho_{\text{Sn}} S_{\text{Sn}}}{L_{\text{Sn}}}$$

But $L_{\text{Fe}} = L_{\text{Sn}} = L_0 \cong L$ since Fe, Sn and the total scattering are predominantly elastic. Then the above becomes

$$\begin{aligned} S &= \frac{1}{\rho} (\rho_{\text{Fe}} S_{\text{Fe}} + \rho_{\text{Sn}} S_{\text{Sn}} + \frac{L_0}{L_L} \rho_L S_L) \\ &\cong \frac{1}{\rho} (\rho_{\text{Fe}} S_{\text{Fe}} + \rho_{\text{Sn}} S_{\text{Sn}} + \frac{L_0}{L_0 + \Delta L} \rho_L S_L) \\ &\cong \frac{1}{\rho} (\rho_{\text{Fe}} S_{\text{Fe}} + \rho_{\text{Sn}} S_{\text{Sn}} + (1 - \frac{\Delta L}{L_0}) \rho_L S_L) \\ &\cong \frac{1}{\rho} (\rho_{\text{Fe}} S_{\text{Fe}} + \rho_{\text{Sn}} S_{\text{Sn}} + \rho_L S_L) \end{aligned}$$

assuming $\Delta L/L_0$ is small. At 100K, $\Delta L/L_0 \cong 0.1$ so that the phonon scattering is becoming quasi-elastic with the higher temperature. At 50K, $\Delta L/L_0 \cong 0.3$, but ρ_L is reduced enough to make $\rho_L S_L$ small.

The linearity of the higher temperature plots is probably indicative of this and of being able to neglect the phonon drag

contribution. The phonon drag contribution is also expected to decrease with increasing impurity scattering as mentioned in section 1.5.

Recalling equation (1.17),

$$S = S_{\text{Sn}} + \frac{\rho_{\text{Au-Fe}}}{\rho} (S_{\text{Au-Fe}} - S_{\text{Sn}})$$

the intercept of the plots at $1/\rho = 0$ is interpreted as the characteristic thermopower of Sn in Au-Fe. The trend of the plots is for S_{Sn} to increase positively with temperature from a very small value, <0.5 V/K at temperatures of 25K and below. There is nothing here to disagree with the data of MacDonald et al. (1962) for Sn impurities in pure Au. (See Figure 1.5). Experimental scatter is enough to make really accurate determination of S_{Sn} versus temperature impossible.

Using a formula given by MacDonald (1962a), one can make a guess for the characteristic thermopower at low temperatures

$$S = \frac{\pi^2 k^2 T}{3eE_F}$$

At $T = 6\text{K}$, use of this formula gives $S = -0.03\mu\text{V/K}$ for impurities in Au, a small number that agrees with our results. At 100K this formula gives $S \cong -0.5\mu\text{V/K}$ which agrees in magnitude with our results but unfortunately not in sign.

Suggestions for Further Experiments

If a consistent process for making Au-Fe alloys could be

found, there are interesting things one could do. For more concentrated Fe content the Zeeman energies of the impurities become larger so that at low enough temperatures, the spin-flip scattering would be significantly inelastic. See Figure 1.3 for the depressions of the Lorentz ratio for higher Fe concentrations, indicative of inelastic scattering.

One could also look for deviations from the Nordheim-Gorter rule much as one looks for deviations from Matthiessen's rule. At high temperatures this would be easier to do with binary alloys since the alloying problem would be lessened. At low temperatures, the phonon contribution dies, and a ternary alloy is necessary. As mentioned in section 1.6 on the basis of the two band model with anisotropic scattering, the thermopower is expected to obey a Nordheim-Gorter-like rule but with a different interpretation of the intercept for dilute alloys.

The process here described for putting Sn into the Au-Fe wire could be used to make Au-Sn alloys. The characteristic thermopower of the Sn in Au could be obtained from Nordheim-Gorter plots at various temperatures. The literature has few such measurements. Here the phonon drag peak would not be swamped by the Fe scattering and the rule might fail at this temperature.

APPENDIX I

THE DIFFUSION OF Sn IN SOLID Au

Ceresara et al. have solved the diffusion equation,

$$\frac{\partial c}{\partial t} = D \nabla^2 C_1$$

for the case where the solute metal is deposited on the surface of a wire of radius a at $t = 0$ and left to diffuse in. Their results are summarized in Figure I.1, where

$$X = r/a \quad \text{and} \quad Y = \frac{C(X, \tau)}{C_f}$$

At $\tau = Dt/a^2 = 0.2$ one sees that the concentration is almost uniform throughout the specimen.

The value of D for the Au-Sn system was not to be found in either Jost's book (1960) or in the journal, Diffusion Data. At $T = 850C$ similar systems have diffusion coefficients as follows:

$$D(\underline{\text{Au-Cu}}) = 1.36 \times 10^{-9} \text{ cm}^2/\text{sec} \quad (\text{Diffusion Data. 1967. 1. No. 1, 8.})$$

$$D(\underline{\text{Cu-Sn}}) = 1.93 \times 10^{-10} \text{ cm}^2/\text{sec} \quad (\text{ibid. 1967. 1. No. 3, 18.})$$

$$D(\underline{\text{Au-Sb}}) = 1.16 \times 10^{-8} \text{ cm}^2/\text{sec} \quad (\text{ibid. 1968. 3, 127.})$$

For the smallest diffusion coefficient, $D(\underline{\text{Cu-Sn}})$, with 0.08 mm wire, $\tau = 0.2$ corresponds to $t = 1.6 \times 10^4$ seconds = 0.18 days. Thus a 24 hour treatment at 850C should be enough time to

achieve uniform distribution of Sn throughout the Au wire used in this experiment.

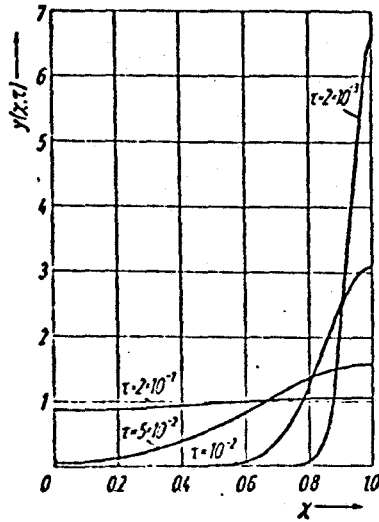


Figure I.1 Concentration vs. radial position for various times for diffusion into a cylinder from the surface.

APPENDIX II

THE VALIDITY OF MATTHIESSEN'S RULE IN TERNARY ALLOYS

Stewart and Huebener (1970) have carefully studied deviations from Matthiessen's rule for Au with various solutes. Some of their results are shown in Figures II.1 and II.2. $\Delta(T)$ is the deviation from Matthiessen's rule and ρ_j is the residual resistivity. For non-magnetic impurities the worst case of $\Delta(T)/(\rho_j + \rho_L(T))$ is about 8% for Au+1% Pt at 40K for alloys with less than 0.5% impurity concentration.

From Stewart's curves one sees that Matthiessen's rule fails most severely when the ideal lattice resistivity, ρ_L , is of the same order of magnitude as the residual resistivity. This is quite a general result and has been discussed by Kohler (1949a) and Ziman (1960) where from a variational principle one expects

$$\rho - (\rho_1 + \rho_2) \leq \beta_1 \beta_2 \frac{\rho_1 \rho_2}{\beta_1 \rho_1 + \beta_2 \rho_2}$$

where β_1 and β_2 are small, ρ is the actual resistance and ρ_1 and ρ_2 are the resistances of the two scattering mechanisms taken separately. This is referred to as the Kohler-Sondheimer-Wilson equation in the literature.

Stewart and Huebener also found a sharp addition to this peak for low concentrations of impurity which could not be fitted to an equation of this type. They attributed this to

higher order terms in the Boltzmann equation as discussed by Sondheimer (1950).

For Fe impurities in Au, Domenicali and Christensen (1961) have studied the temperature dependence of the resistivity over a wide temperature range as shown in Figure II.3. At the higher temperatures there is a small hump of about 5% magnitude in the resistivity occurring at lower temperatures for lower Fe concentrations. Again this is quite consistent with the general theory of deviations from Matthiessen's rule. Extrapolating down in concentration to Fe in Au with a residual resistance ratio of .148, the peak should occur at around 60K.

At low temperatures for dilute alloys of Fe in Au there is the famous resistance minimum which has been well studied in the literature. As Kondo (1964) pointed out, this results not from departures from Matthiessen's rule but from temperature dependent scattering. Kopp (1969) measured the resistivity of Au+.03 at .% Fe finding about a 2% minimum relative to the resistivity at 4.2K at around 9K. Starting at temperatures slightly below the minimum the resistivity from which the ideal resistivity was subtracted showed a small deviation from the expected $\ln T$ behavior. This was attributed to deviations from Matthiessen's rule and higher order effects in the Fe resistivity. The error

$$\rho = (\rho_0 + \rho_L)$$

had about cancelled itself out at 11K due to the rise in resistivity up from the minimum. Kopp's measurements ended at this temperature. The deviations would most likely reach the same magnitude as Domenicali's 0.14% alloy but at a lower temperature, about 60K, as mentioned above.

Loram et al. (1970) found that deviations from Matthiessen's rule in dilute magnetic alloys could be satisfied as a relation of the form

$$\frac{\beta_L \rho_L \beta_i \rho_i}{\beta_L \rho_L + \beta_i \rho_i} ; \beta_i \alpha \rho_i^{-0.45}$$

Therefore in a $\text{Cu}_{90}\text{Au}_{10}$ alloy where ρ_i is large, β_i is small and when the ρ_L term dominates, the error is very small. Figure II.4 shows the extension of the approximate $\ln T$ behavior to much higher temperatures than pure Au-Fe and Cu-Fe alloys. Impurity resistivity is swamping out the deviations from Matthiessen's rule due to the lattice resistivity. Their Au concentration is much higher than any Sn concentrations in the present experiment and these results may not hold for dilute alloys.

It is probably unlikely that a more dilute ternary alloy of Au-Fe-Sn would exhibit any startling deviations from Matthiessen's rule. The Kohler-Sondheimer-Wilson relation seems to give reasonable agreement for most binary alloys and can be extended easily to ternary alloys. In the present experiment Matthiessen's rule probably holds to within 5%.

This was used for the error bars in Figures 3.2, 3.3, and 3.4.

For the intrinsic lattice resistivity of pure Au the data of White and Woods (1959) were used. It was divided by the resistivity at 295K and added on to the residual resistance ratio of the Au-Fe-Sn alloys to obtain the total resistivity as a function of temperature.

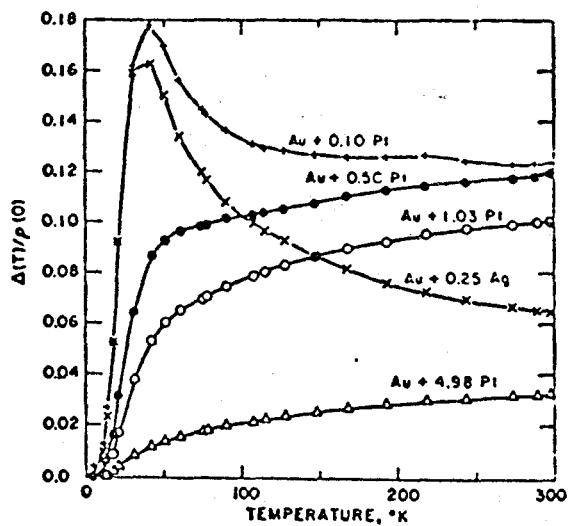


Figure II.1

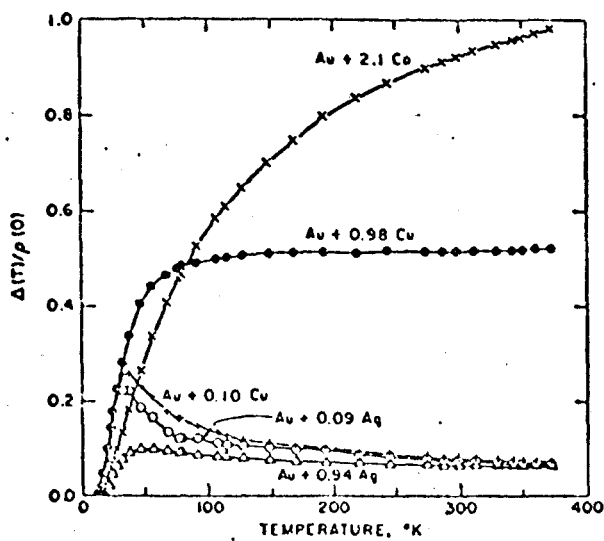


Figure II.2 $\Delta(T) / \rho_0(0)$ versus temperature for various gold alloys

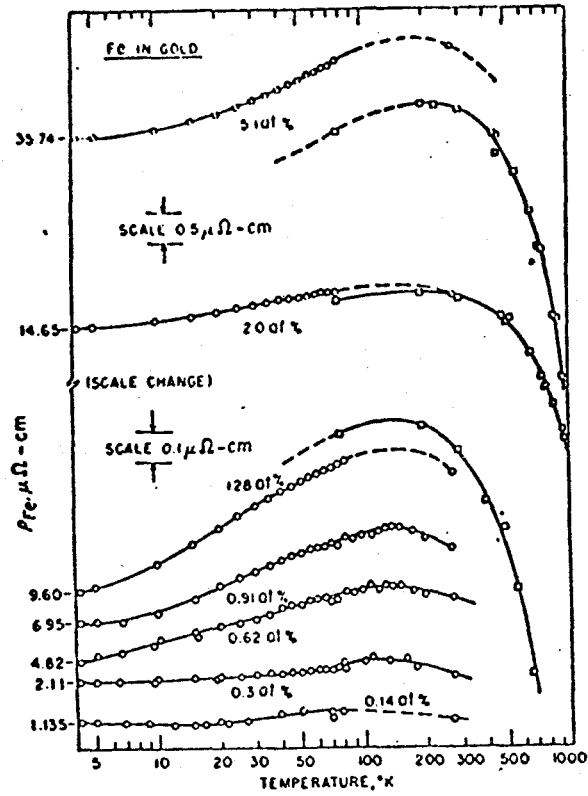


Figure II.3 Temperature dependence of the solute contribution Fe to the resistivity of gold-iron alloys in the range 4° to 1000°K

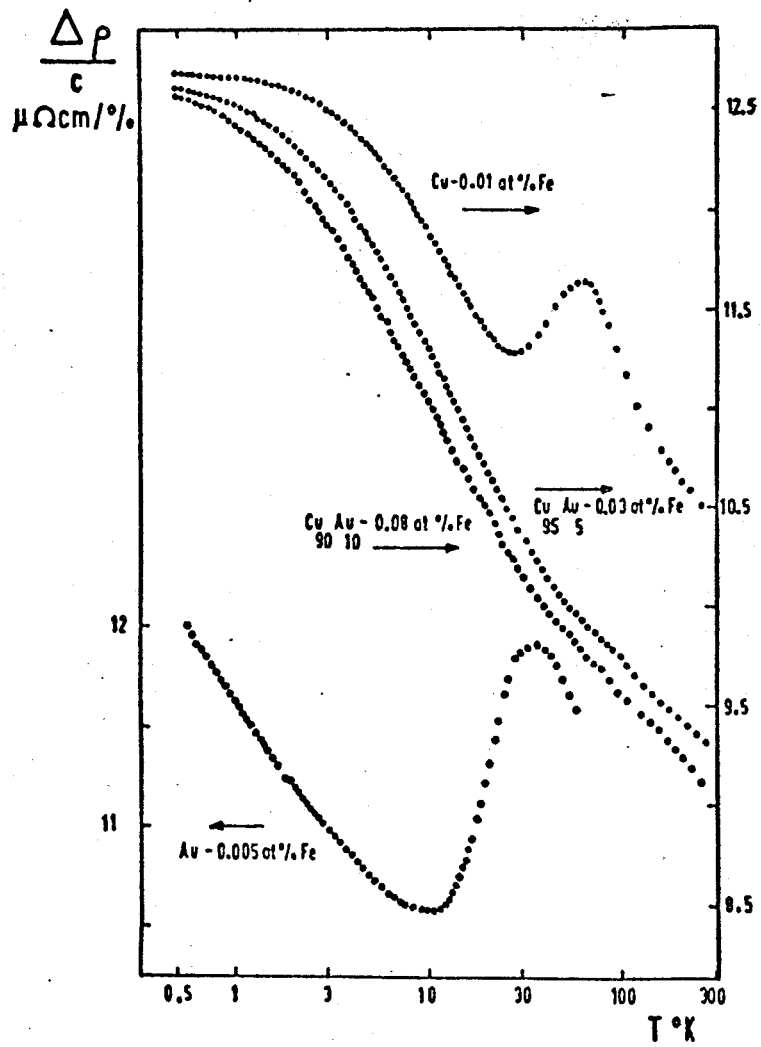


Figure II.4 Deviations from Matthiessen's rule versus temperature for various alloys

APPENDIX III

THE EFFECT OF SUPERCONDUCTING Pb

IMPURITIES ON THE MAGNETOTHERMOPOWER

AND MAGNETORESISTANCE OF PURE Au AND Au-Fe ALLOYS

While studying the magnetic field dependence of the thermopower of dilute alloys of Fe in Au, Walker (1971) observed an interesting effect for small fields. The percentage change in thermopower with applied field is shown in Figure III.1. For small enough fields Walker argued that $\Delta S/S$ versus H should be parabolic in H . The dashed lines in the figure show the good parabolic fit for higher fields and the continuation to smaller fields. One notes the rather sharp deviation from parabolic behavior at these lower fields. Taking the midpoint, H_c , of this sharp transition, Walker made the plot of H_c versus temperature shown in Figure III.2.

For zero field the critical temperature extrapolates to around 7.2K. Walker reasoned that this effect was due to a superconducting transition in Pb impurities in his alloy since the superconducting transition temperature of Pb is 7.19K. Since the thermopower in this region is dominated by the Fe impurities, Walker explained this effect in terms of the Nordheim-Gorter rule and change in resistivity of the wire as the suspected Pb impurities went normal. About 3 ppm of Pb impurity would explain this effect, a reasonable figure in light of an NRC spectrographic analysis of a wire from the same

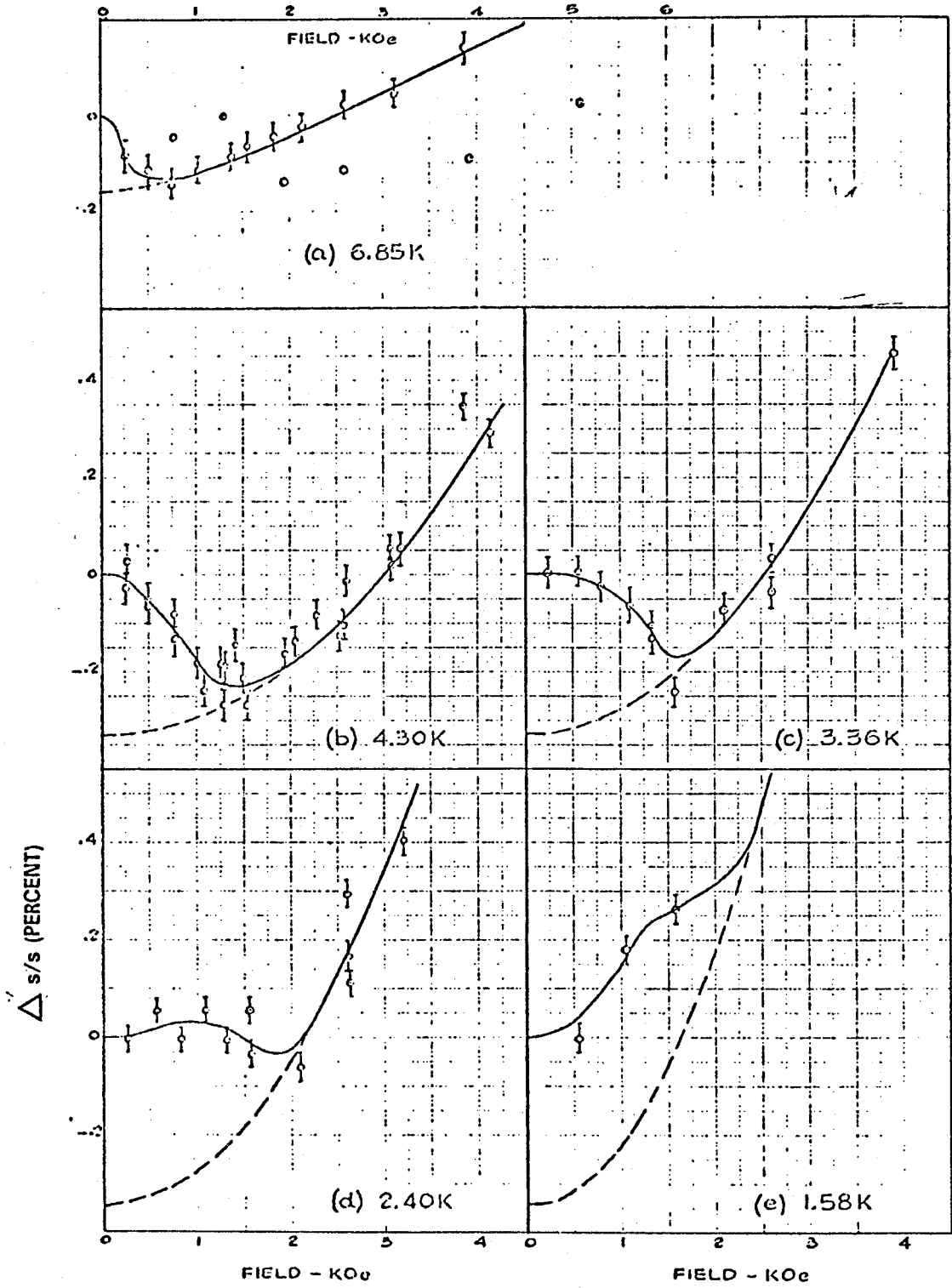


Figure III.1 Percentage change in thermopower versus magnetic field in Au + 0.03 at % Fe at low fields

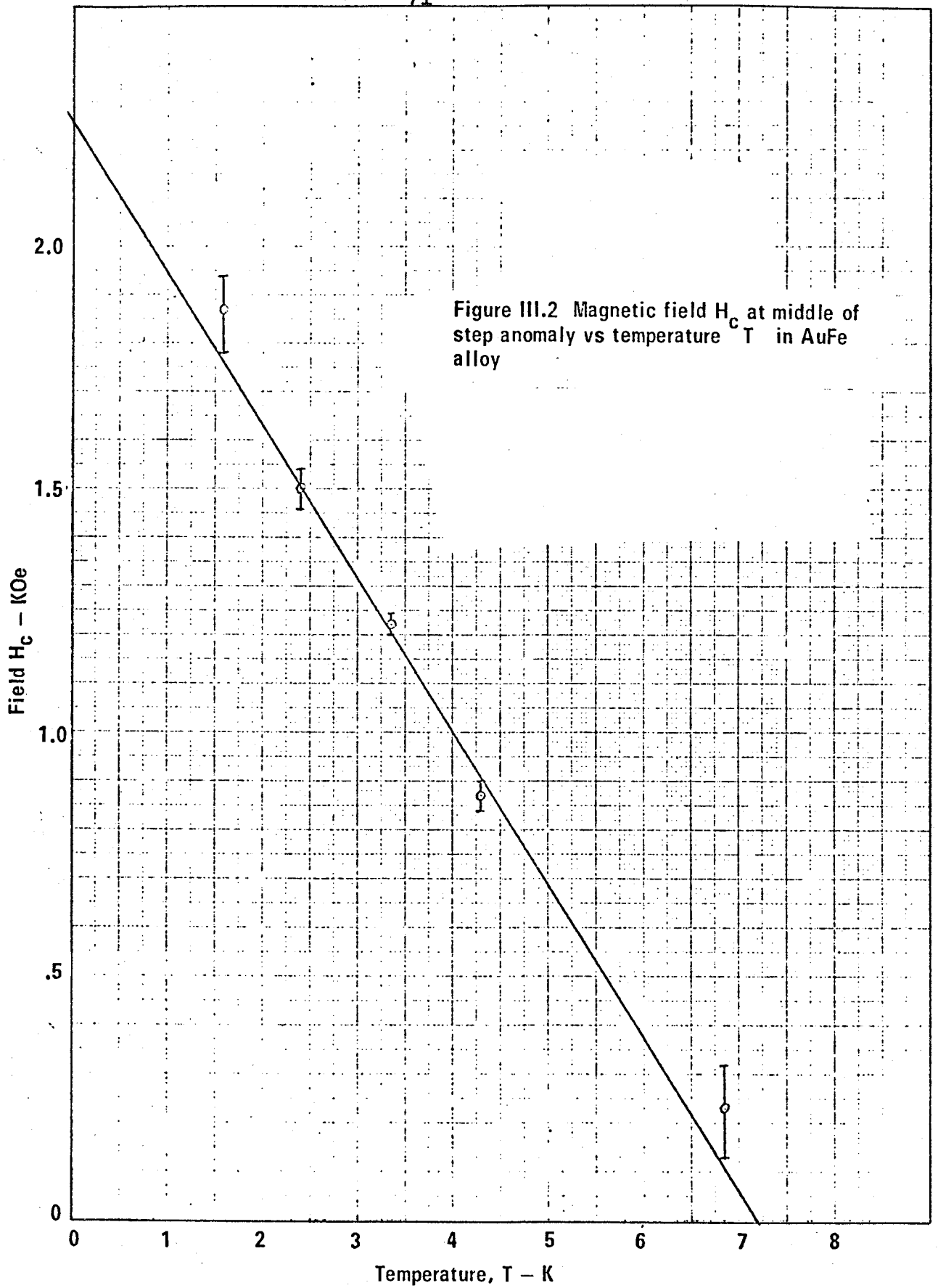


Figure III.2 Magnetic field H_c at middle of step anomaly vs temperature T in AuFe alloy

spool indicating a Pb concentration of about 15 ppm.

To explain why the Pb should have a superconducting state Walker assumed the Pb to be present in the form of small occlusions. Since Pb is almost completely insoluble in Au below 500C, this is quite possible. Upon annealing, the alloy would become two phase, the Pb perhaps separating out into small regions.

To test Walker's hypothesis that the resistivity changed as a result of a superconducting transition, the magneto-resistance of various alloys was measured. In addition, it was thought that such measurements would yield interesting information about the minimum size necessary for superconducting behavior and general size effects as a fraction of magnetic field. When the size of the occlusions is reduced to the order of the coherence length, the critical field should increase in magnitude.

All the specimens were in the form of 0.08 mm diameter wires mounted essentially in a transverse magnetic field. The 55KG Nb-Ti superconducting magnet was from Oxford Instruments. It was used at large fields with an Hewlett Packard (HP) HP6387A DC power supply. For small fields, less than 6KG, a reversible bipolar operational power supply, Kepco BOP 72-5 m, was used in order to sweep the field through zero and minimize hysteresis effects. Voltages were measured using an HP419A DC Null voltmeter and Tinsley 5590B potentiometer feeding an HP7030A X-Y recorder. Specimen current was supplied by an

HP6186B DC current source.

Figures III.3 and III.4 show the low field magnetoresistance traced directly from the plotter trace for two Au+0.03 at.%

Fe alloys, one a small piece from Walker's specimen used to obtain Figure III.1, the other from a spool of Johnson Matthey thermocouple wire dated April 1971 used to make the Au-Fe-Sn alloys described earlier in this thesis. The temperature was around 4.2K. One is immediately struck by the absolute absence of anything resembling a superconducting transition anywhere near the 0.25% magnitude observed by Walker. Apparently Walker's explanation was wrong.

Undaunted by this, we attempted to put Pb into Au wires, arriving finally at the procedure described in Chapter II of this thesis. Nothing in the way of a superconducting transition was observed in the raw magnetoresistance plots. The results of these experiments is summarized in Figure III.5. Sample I is Cominco 99.9999% pure Au. Sample II is the above with around 1300 ppm added Pb impurity snatched out of the oven at 850C and called unannealed. Sample III is Sample II subjected to the more gradual cooling of turning off the furnace. This figure is in the form of a Kohler plot, successful in explaining the effect of impurities on the magnetoresistance of many metals. Kohler's rule may be stated as

$$\Delta R/R = F\left(\frac{H}{\rho}\right) ; F(X) \text{ is a function of } X. \rho \text{ is electrical resistivity.}$$

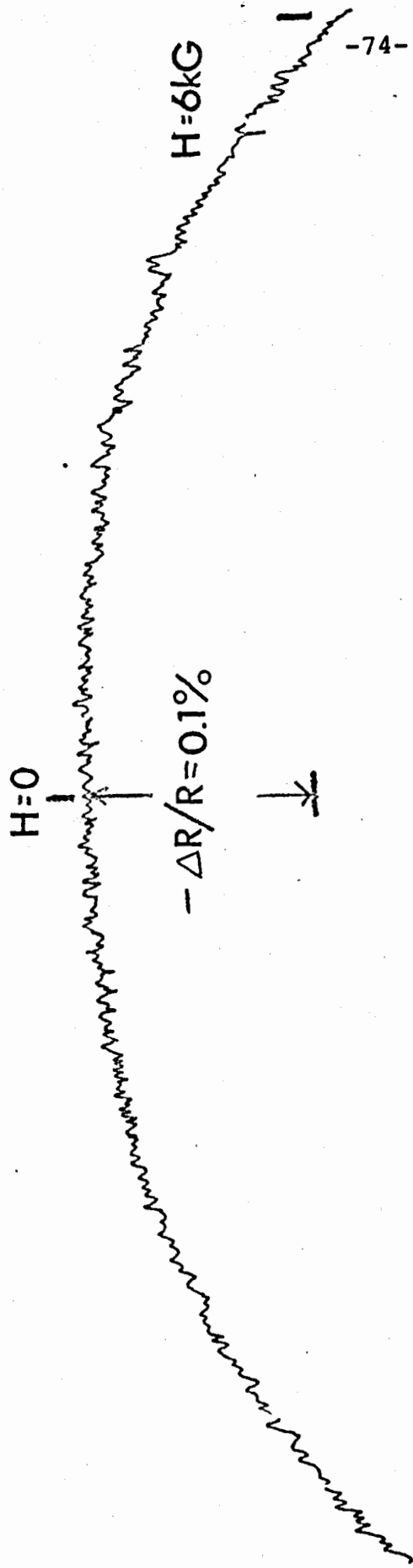


Figure III.3 Magnetoresistance of Walker's Au + 0.03 at % Alloy at $T = 4.2\text{K}$

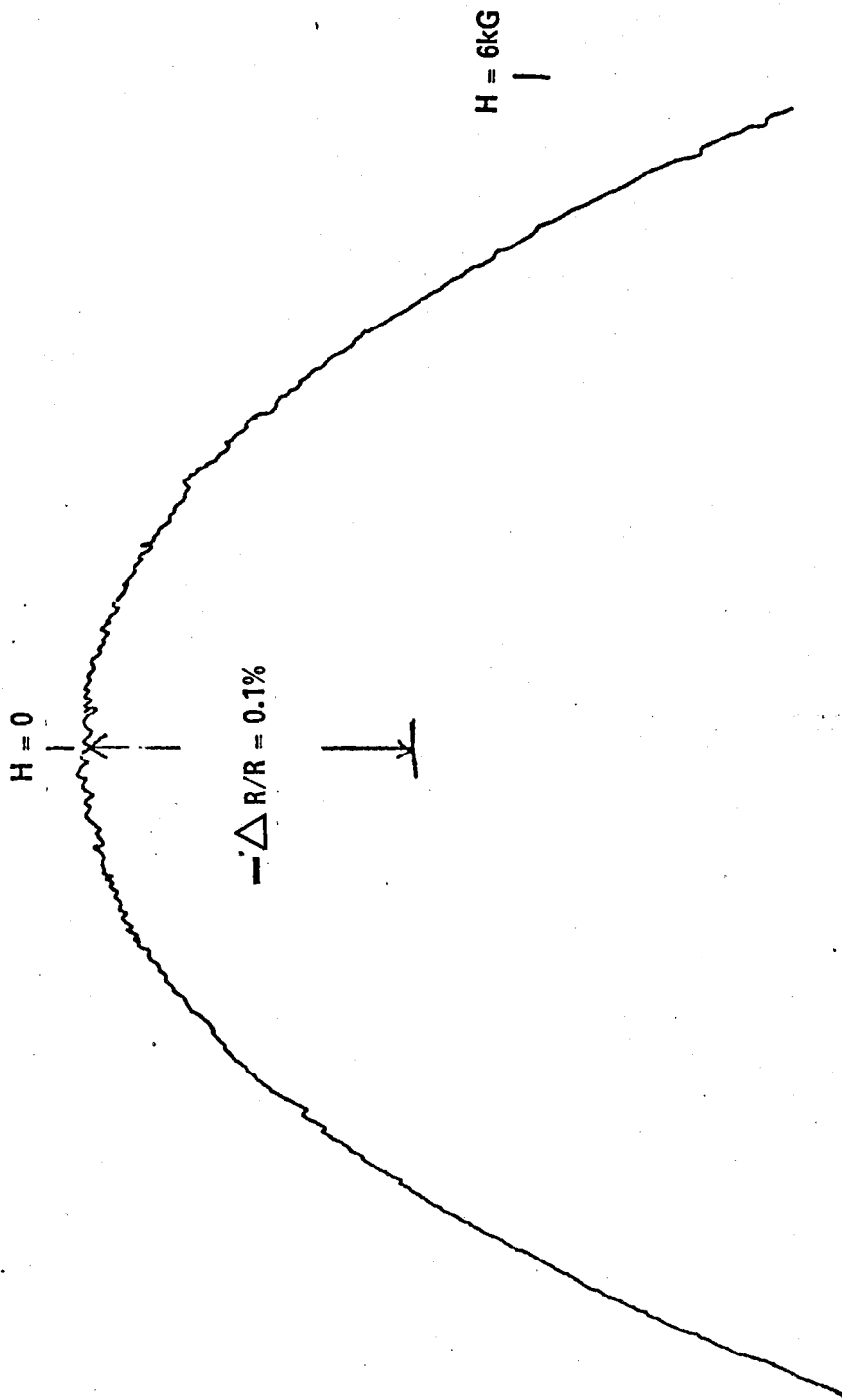
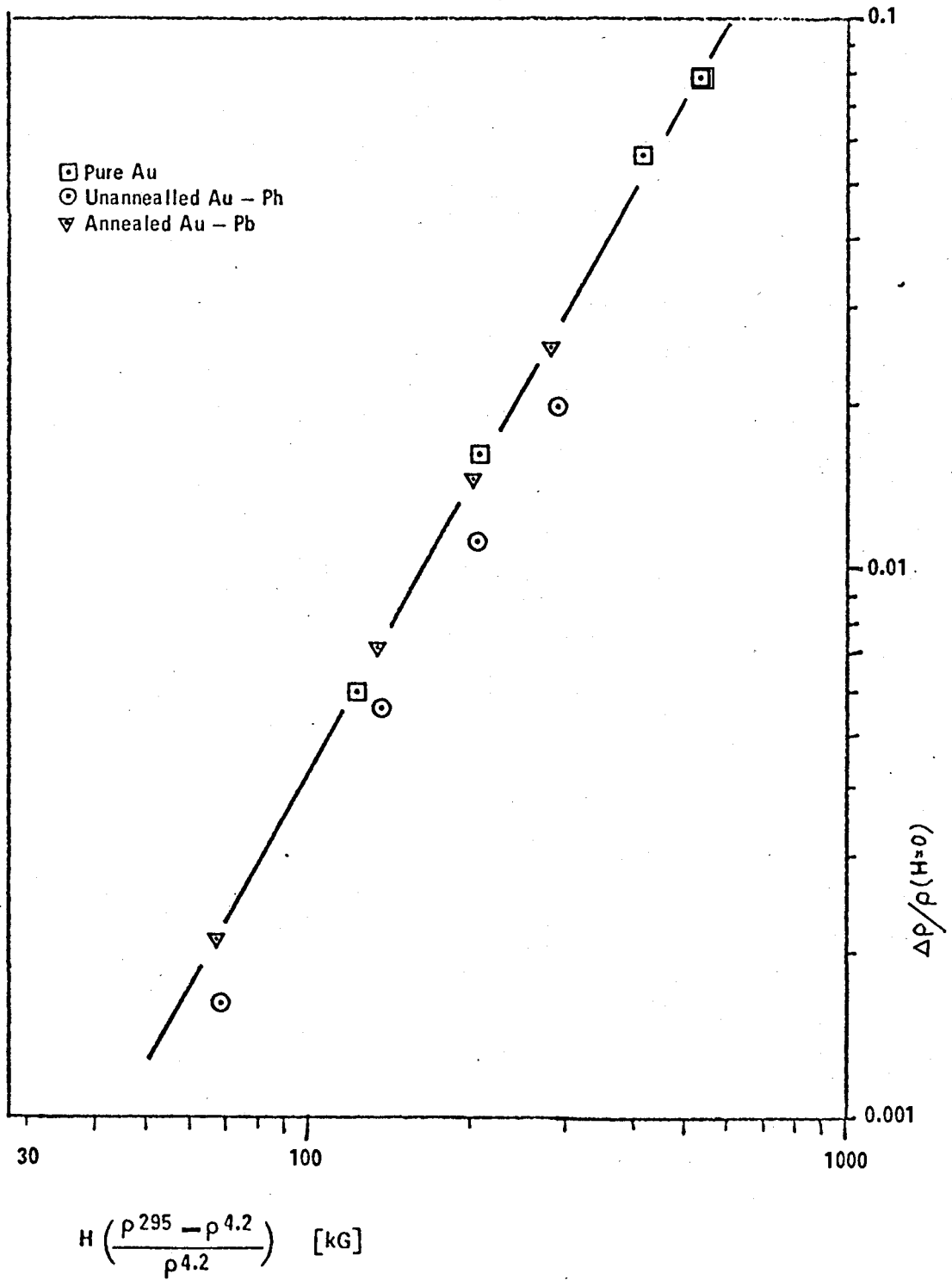


Figure III.4 Magnetoresistance of April 1971 Au + 0.03 at % Fe alloy at $T = 4.2\text{K}$

Figure III.5 Reduced Kohler plot of Au and Au-Pb alloys



The ratio H/ρ is important, not the absolute value of the magnetic field. Note that Kohler's rule is well satisfied in this experiment for the annealed specimen. Even subject to a slow anneal, the Pb impurities exhibit no unusual behavior.

Well, there was nothing left to do but measure the magnetothermopower of Walker's original specimen (minus the small piece chopped off to perform the magnetoresistance experiment). The cryostat used was very similar to that described in Chapter II but with Ag normal voltage leads. Ag normal has a very small magnetothermopower and thermopower at low temperatures and so is well suited for the present purpose. A Keithley 148 nanovoltmeter fed the X-Y plotter. About a $10\mu\text{V}$ thermoelectric voltage was set up and the magnet swept from 6KG north through zero to 6KG south. Figure III.6 is traced directly from the plot. The width of the plot is attributed to an interference effect caused by the second harmonic of the 93 HZ voltmeter chopping frequency beating with the third harmonic of the 60 HZ line frequency. The slight assymetry is probably due to slow drift in the He level causing temperature drifts as the plot took over half an hour to make. The results here on Walker's very own specimen indicate either that he was observing an apparatus effect or that time has altered his specimen.

About 1100 ppm Pb was added to Au+0.02 at .% Fe thermocouple wire. The magnetothermopower was measured and at low fields nothing resembling Walker's results was found as is shown in Figure III.7, traced directly from the experimental

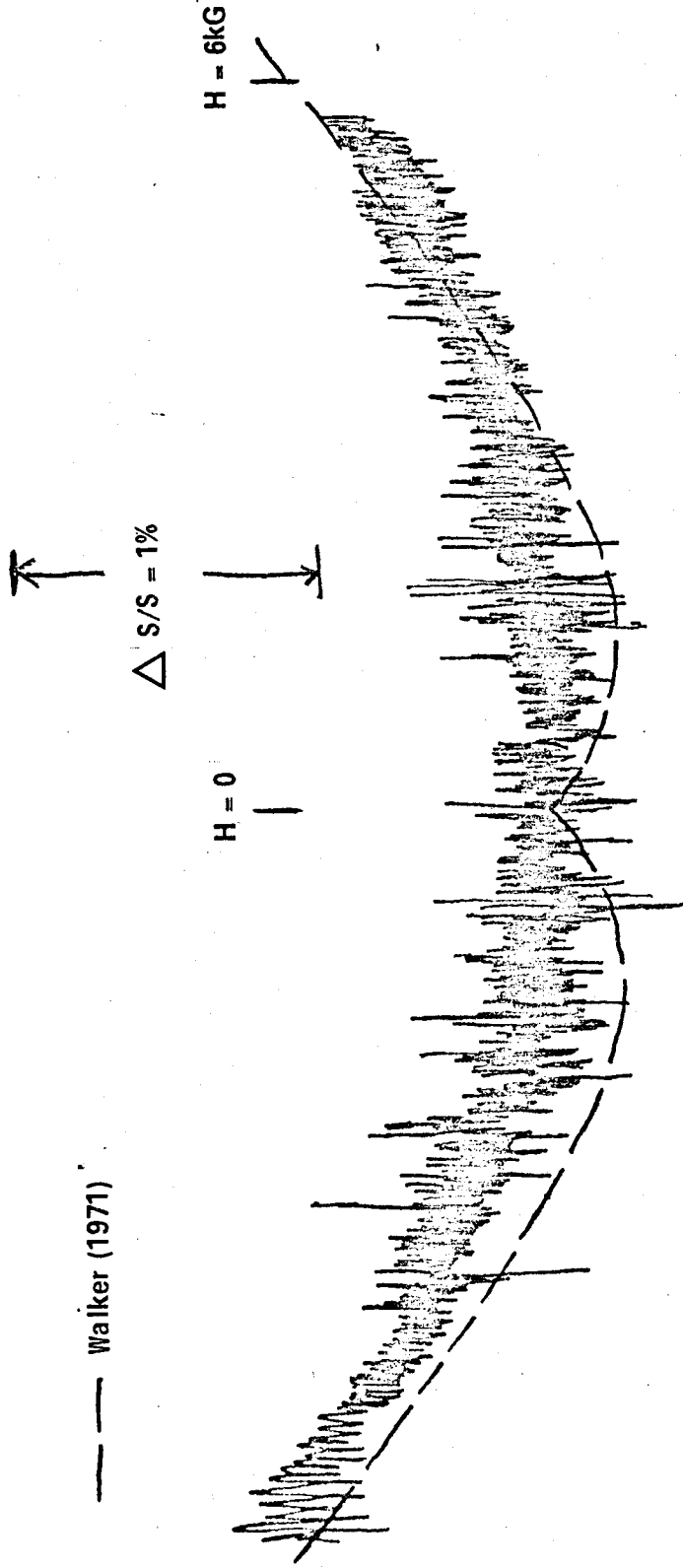
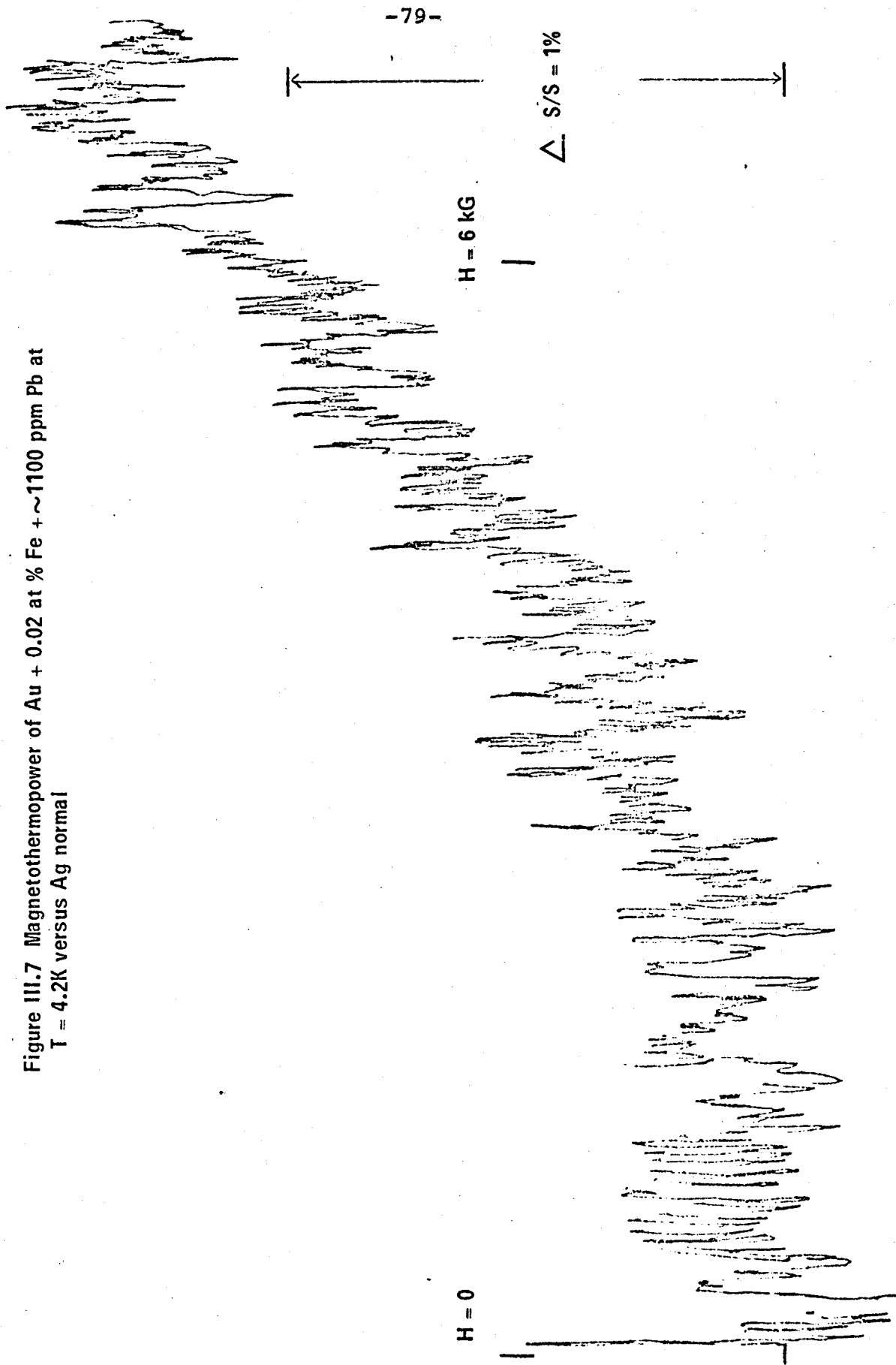


Figure III.6 Magnetothermopower of Walker's Au + 0.03 at % Fe alloy at $T = 4.2K$ versus Ag normal

Figure III.7 Magnetothermopower of Au + 0.02 at % Fe + ~1100 ppm Pb at
T = 4.2K versus Ag normal



plot.

In conclusion one can only state that while Walker definitely measured something, it was not to be found again. It also appears that getting Pb to separate out of Au into small occlusions is not easy for concentrations around 1000 ppm Pb as evidenced by the regular behavior of the Kohler plot, Figure III.5. If such a specimen full of tiny Pb occlusions could be prepared it would be interesting to study the thermal and electrical scattering and general superconducting behavior.

LIST OF REFERENCES

- Berman, R. Brock, J.C.F. and Huntley, D.J. Cryogenics.
4, 233.
- Berman, R. and Kopp, J. J. Phys. F: Metal Phys. 1, 457.
- Blatt, F.J. 1968. Physics of Electronic Conduction in Solids
(McGraw-Hill, New York).
- Blatt, F.J. and Lucke, W.H. 1967. Phil. Mag. 15, 649.
- Ceresara, S., Federighi, T. and Pieragostini, F. 1966.
Phys. Stat. Sol. 16, 439.
- Christian, J.W., Jan, J.P., Pearson, W.B. and Templeton, I.M.
1958. Proc. Roy. Soc. A245, 213.
- Dugdale, J.S. and Basinski, Z.S. 1967. Phys. Rev. 157, 522.
- Fritzsche, H. 1971. Solid State Communications. 9, 1813.
- Garbarino, P.L. and Reynolds, C.A. 1971. Phys. Rev. B. 4, 167.
- Gold, A.V., MacDonald, D.K.C., Pearson, W.B. and Templeton, I.M.
1960. Phil. Mag. 5, 765.
- Guenault, A.M. 1972. J. Phys. F: Metal Phys. 2, 316.
- Hansen, M. 1958. Constitution of Binary Alloys (McGraw Hill,
New York).
- Jha, D. and Jericho, M.H. 1971. Phys. Rev. B. 3, 147.
- Jost, W. 1960. Diffusion in Solids, Liquids, Gases (Academic
Press Inc., New York).
- Kittel, C. 1966. Introduction to Solid State Physics (Wiley,
New York).
- Kohler, M. 1949. Z. Phys. 126, 481.
- Kohler, M. 1949a. Z. Phys. 126, 495.

- Kondo, J. 1964. Progr. Theor. Phys. 32, 37.
- Kondo, J. 1965. Progr. Theor. Phys. 34, 372.
- Kopp, J. 1969. Thesis. University of Oxford.
- Loram, J.W., Whall, T.E. and Ford, P.J. 1970. Phys. Rev. B. 2, 857.
- MacDonald, D.K.C., Pearson, W.B. and Templeton, I.M. 1962. Proc. Roy. Soc. A266, 161.
- MacDonald, D.K.C. 1962a. Thermoelectricity (John Wiley and Sons, New York).
- Mott, N.F. and Jones, H. 1936. The Theory of the Properties of Metals and Alloys (Dover reprint 1958, New York).
- Nordheim, L. and Gorter, C.J. 1935. Physica. 2, 383.
- Pearson, W.B. 1961. Solid State Physics (U.S.S.R.). 3, 1411.
- Sondheimer, E.H. 1950. Proc. Roy. Soc. A203, 75.
- Stewart, R.G. and Huebener, R.P. 1970. Phys. Rev. B. 1, 3323.
- Van Peski-Tinbergen, T. and Dekker, A.J. 1963. Physica. 29, 917.
- Walker, C.W.E. 1971. Thesis. Simon Fraser University.
- White, G.K. and Woods, S.B. 1959. Phil. Trans. Roy. Soc. A251, 273.
- Wilson, A.H. 1953. The Theory of Metals (Cambridge University Press, London).
- Ziman, J.M. 1960. Electrons and Phonons (Oxford University Press, London).